

## Review

## A review on the angle of repose of granular materials

Hamzah M. Beakawi Al-Hashemi \*<sup>1</sup>, Omar S. Baghabra Al-Amoudi <sup>2</sup>*Department of Civil and Environmental Engineering, King Fahd University of Petroleum and Minerals, Dhahran 31261, Saudi Arabia*

## ARTICLE INFO

## Article history:

Received 17 September 2017

Received in revised form 28 January 2018

Accepted 2 February 2018

Available online 27 February 2018

## Keywords:

Angle of repose  
Geotechnical  
Granular  
Measurements

## ABSTRACT

The abundance of granular materials and powders that are being used in several fields, along with their broad applications, requires a comprehensive understanding of both their macro- and micro-mechanical behavior. The fabric and structural properties, or the inter-particle properties, such as the angle of repose, do affect the behavior of granular materials. This comprehensive review indicates that the angle of repose of granular material is an essential parameter to understand the micro-behavior of the granular material and, then, to relate it with the macro-behavior. Therefore, this extensive review was prepared about the repose angle theory, its definitions, method of measurements, appropriate applications and the influencing factors.

© 2018 The Authors. Published by Elsevier B.V. This is an open access article under the CC BY license (<http://creativecommons.org/licenses/by/4.0/>).

## Contents

1. Introduction . . . . .	398
1.1. Granular materials . . . . .	398
1.2. Definitions of angle of repose . . . . .	398
2. Measurement of the angle of repose . . . . .	399
2.1. State-of-the practice methods . . . . .	399
2.1.1. Tilting box method . . . . .	399
2.1.2. Fixed funnel method . . . . .	399
2.1.3. Revolving cylinder/drum method . . . . .	400
2.1.4. Hollow cylinder method . . . . .	401
2.1.5. Tilting cylinder method . . . . .	401
2.1.6. Comparison . . . . .	402
2.2. State-of-the-art methods . . . . .	402
3. Applications of the angle of repose . . . . .	403
3.1. Major applications . . . . .	403
3.1.1. Agricultural engineering . . . . .	403
3.1.2. Entomology . . . . .	403
3.1.3. Geotechnical engineering . . . . .	403
3.1.4. Hydrodynamics and sedimentology . . . . .	403
3.1.5. Particle technology and materials science . . . . .	404
3.2. Other applications . . . . .	405
3.3. Calibration of numerical models and simulations . . . . .	406
4. Influential factors . . . . .	407
4.1. Geometrical properties of the particles . . . . .	407
4.1.1. Particle roundness . . . . .	408
4.1.2. Sphericity of particles . . . . .	411
4.1.3. Roughness . . . . .	411

\* Corresponding author.

E-mail address: [g201552950@kfupm.edu.sa](mailto:g201552950@kfupm.edu.sa) (H.M. Beakawi Al-Hashemi).<sup>1</sup> 0000-0002-3991-1712<sup>2</sup> 0000-0001-5078-9204

4.2. Particle size . . . . .	411
4.3. Friction coefficients . . . . .	412
4.3.1. Sliding (Coulomb) friction coefficients . . . . .	412
4.3.2. Rolling friction coefficient . . . . .	412
4.3.3. Angle of internal friction . . . . .	412
4.4. Coefficient of restitution (damping) . . . . .	413
4.5. Number of particles. . . . .	413
4.6. Moisture content and air flow . . . . .	413
4.7. Methods of measurement . . . . .	413
5. Conclusions. . . . .	413
6. Recommendations for future research. . . . .	413
Acknowledgments . . . . .	414
References. . . . .	414

## 1. Introduction

In industrial and engineering applications, the use of granular materials such as powders, seeds, and soils is unavoidable [1]. Therefore, further studies and improvements are currently needed to optimize and facilitate the process of handling and manufacturing bulk granular materials. Such improvements are contingent on the elucidation of the various properties and mechanical behavior of these materials. The challenges of handling and manufacturing granular materials arise when the materials are sheared or disturbed because they will behave as non-Newtonian fluids instead of stable, solid materials [2]. Moreover, the stress distribution in granular materials is not uniform but is distributed along the force chains [3], which depend on the particle contacts and packing arrangement. The flowability of granules is dependent on a set of parameters, one of which is the angle of repose [4]. Therefore, while the angle of repose can be used as an indication of flowability, this angle is controlled by numerous factors and has different definitions, methods of measurement, and applications that are discussed in this review.

### 1.1. Granular materials

While the primary material used in industry is fluid, the second most widely used material is of granular nature [1]. Granular material is a cluster of distinct particles that lose energy when interacting with other particles [5]. Commonly, the particle size determines if a material is considered granular. The minimum particle size of the granular material is 1  $\mu\text{m}$ , and materials with a smaller particle size may be subjected to thermal motion oscillations. For instance, soils are called granular, coarse-grained, or cohesionless when >50% of the weight of the soil is sand and gravel that have sizes ranging from 0.07 to 5 mm and 5 to 75 mm, respectively [6]. Granular soils are often non-plastic and will not form coherent matter when wet. The permeability of the granular soil is high to moderate due to the presence of voids. Nonetheless, a small amount of fine material, such as clay, when present in the granular soil may significantly change the bulk behavior and properties of the soil. The mechanical behavior of the granular material is affected by its structure and fabric and the effective applied stress. Factors like density, anisotropy and particle arrangement will determine the material structure, while the particle shape, size, contacts, and distribution will control the fabric. The particle size gradation of granular soil can be used to indicate its origin [6]. Poorly-graded soils are usually found in alluvial and aeolian deposits, while well-graded soils are found in glacial deposits. However, the shape and size of a granular material have a considerable effect on its behavior and properties, such as the void ratio, crushability, compressibility, deformation, strength, relative density, internal friction and angle of repose.

### 1.2. Definitions of angle of repose

The definition of the angle of repose should be application- and behavior-specific. The different types (static and dynamic) and

descriptions of the angle of repose are associated with specific applications and the corresponding behavior (i.e., flowability, friction, etc.). Therefore, the objectives of studying and determining the angle of repose of any granular material should be predetermined so that an appropriate and relevant definition can be adopted in the context of those objectives. Physically, the angle of repose can be defined as the angle that differentiates the transitions between phases of the granular material [7]. One of the most commonly used definitions of the angle of repose is the steepest slope of the unconfined material, measured from the horizontal plane on which the material can be heaped without collapsing [8].

For powders, which can be defined as small-sized granular materials subject to cohesion and suspension in a gas, the definition of the angle of repose is frequently linked with the Hausner ratio or the tapped-to-bulk density ratio [9], and the powders will flow at angles greater than the angle of repose [10]. The angle of repose can also indicate the cohesiveness of the granular material [11], referring to the Carr classification of flowability [12,13] shown in Table 1. However, for cohesive materials, the angle of repose is hard to obtain. Hence, indirect methods are often used, such as the angle-composition plot method [14], which is based on mixing the cohesive material with granular material and plotting the composition against the respective angle of repose to indirectly obtain the angle of repose of the cohesive material.

In soil mechanics, Karl Terzaghi defined the angle of repose as a special internal friction angle that is acquired under extreme (loosest state) conditions [15]. Additionally, it may be defined as the angle of maximum slope inclination at which the soil is barely stable [16]. Geotechnically, the primary application of the angle of repose is in the determination of slope stability and design of retaining structures [17]. Generally, the angle of repose is related to the static friction coefficient and the angle of internal friction. In the literature, the angle of repose is often assumed to be equal to the residual internal friction angle or the constant volume angle in a critical state [18–20]. This assumption is not always correct because the behavior of granular soil under low confining pressure is considerably different than that under zero confining pressure [21]. Moreover, for fine and dry granular material with a small angle of repose and a particle size <5  $\mu\text{m}$ , no defined relationship exists between the repose and internal friction angles [22]. As per the classical Coulomb's theory of the friction/material [23], the angle of internal friction is approximated as the arctan of the maximum static friction coefficient (i.e., the angle of repose). This approximation is based on

**Table 1**  
Carr classification of flowability of powder based on repose angle [12].

Description	Repose Angle
Very free-flowing	<30°
Free flowing	30–38°
Fair to passable flow	38–45°
Cohesive	45–55°
Very cohesive (non-flowing)	>55°

some assumptions such as the frictional force is independent of the contact area, and it is linearly related to the normal force, and the heaped materials form perfect conical shapes which is not always the case [24]. However, it was reported that a decrease in normal forces could be associated with an increase in friction forces which contradicts with the Coulomb's theory [25].

Numerous factors, such as the angle of internal friction, grain size and shape, density, moisture content, interface friction angle, stratification, roughness of the base at which the material is heaped, segregation, pull-out velocity of the hollow cylinder (a measurement instrument for the angle of repose), mass of the material, pouring height, morphology of the material, and addition of solvents, can affect the angle of repose, as shown later in this review. The angle of internal friction is the angle between the normal and resultant forces that occur at failure due to shear stresses within a substance, while the interface friction angle is used to determine the skin frictional resistance between different substances. Moreover, when the interface friction angle is determined between two surfaces of the same type of material, it can be proportionate to the peak angle of internal friction by a ratio between approximately 0.2 and 1.0 [26,27]. In general, the angle of repose ranges from 0° to 90°; while for sand, it ranges from 30° to 35° [28,29], as reported in Table 2 [30].

## 2. Measurement of the angle of repose

Analogous to the definition of the angle of repose, the method of measurement should be selected based on predefined objectives and for a specific material and application. Although there are different methods and guidelines available in the literature, the methods are neither standardized nor consistent [31]. The existing methods measure both the static and dynamic angle of repose, as will be discussed later in this section. However, for each method, instruments of different size and scale are used.

### 2.1. State-of-the practice methods

Originally, the angle of repose was physically measured in the eighteenth century by Coulomb [23]. The angle of repose can be determined by numerical methods such as the discrete, or distinct, element method (DEM), as depicted in Fig. 1, electrical capacitance tomography (ECT), and magnetic resonance imaging (MRI) [32,33]. However, in the DEM, rather than obtaining the angle of repose, this angle is used to calibrate the numerical models, as shown later in this review. These methods are especially useful for measurement of the dynamic angle of repose,

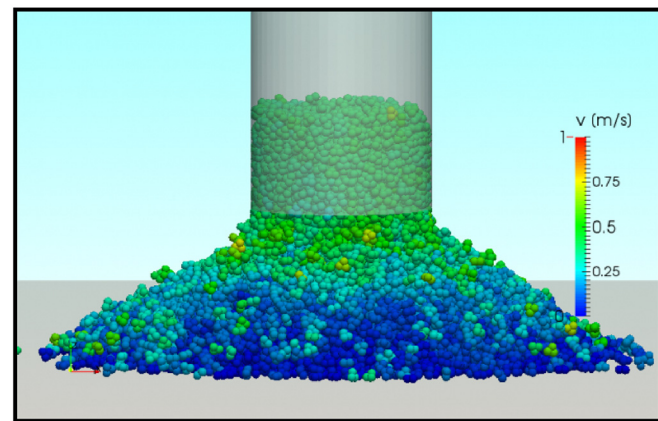


**Fig. 1.** DEM simulation of static angle of repose ([www.Simphysics.com](http://www.Simphysics.com)).

although such techniques require further development before application to natural materials [34]. The most common methods used to determine the angle of repose physically are presented below.

#### 2.1.1. Tilting box method

The tilting box method is suitable for cohesionless, fine-grained materials with a grain size <10 mm. The box must contain at least one transparent side; the granular material is placed on the base of the box, and then the box is tilted gradually at a rate of 18°/min. The angle of repose is then measured as the tilting angle at which the material begins to slide [7,35], as shown Fig. 2. However, this method provides the coefficient of static (sliding) friction rather than the angle of repose.

#### 2.1.2. Fixed funnel method

In the fixed funnel method, the granular materials are poured from a funnel at a certain height onto a selected base with known roughness properties. The funnel is either fixed or raised slowly while the conical shape of the material heap is forming to minimize the effect of the falling particles. The pouring of the material is stopped when the heap reaches a predetermined height or width. Then, the angle of repose is measured by the inverse tangent (arctan) rule at which the average radius of the formed conical shape and the maximum height of the heaped material are measured, and then the angle of repose is determined as the arctan of the maximum height to average radius ratio. This test is the most frequently used for different sizes and combinations of funneling methods (e.g., internal flow funnel and external flow funnel or a combination of both). Depending on the funneling method, two types of the angles of repose can be obtained: the external (or poured) angle of repose and the internal (or drained) angle of repose [36]. Cho, Dodds and Santamarina [37] noticed that the internal angle of repose is significantly greater than the external one, as shown in Fig. 3. This difference is due to the cross-section of the material that is gradually reducing in the case of the internal funnel as the sliding particles consolidate, increasing the coordination number (the inter-particle contacts) [37].

Using the fixed funnel method, Nelson [38] measured the angle of repose of sulfathiazole materials for a pharmacology application. In this case, the angle of repose was found to be equal to the angle of internal friction of the material only when the grains had a uniform shape and size, and the uncertainty in the measurement was reported as 1.0°. Miura, Maeda and Toki [39] introduced a funnel-type device to determine the angle of repose in which the pile of soil was formed on a cylindrical pedestal with a depression. They studied the relationship between the angle of repose and the angle of internal friction, examining different factors such as the roughness of the base, density of the soil, mean grain size, grain shape, dilatancy and lifting speed of the funnel. Their results indicate that the angle of repose tends to decrease

**Table 2**  
Typical values of angle of repose [30].

Material (condition)	Angle of repose
Ashes	40°
Asphalt (crushed)	30–45°
Bark (wood refuse)	45°
Chalk	45°
Clay (dry lump)	25–40°
Clover seed	28°
Coconut (shredded)	45°
Coffee bean (fresh)	35–45°
Earth	30–45°
Flour (corn)	30–40°
Flour (wheat)	45°
Granite	35–40°
Gravel (crushed stone)	45°
Gravel (natural w/ sand)	25–30°
Malt	30–45°
Sand (dry)	34°
Sand (water filled)	15–30°
Sand (wet)	45°
Snow	38°
Wheat	27°

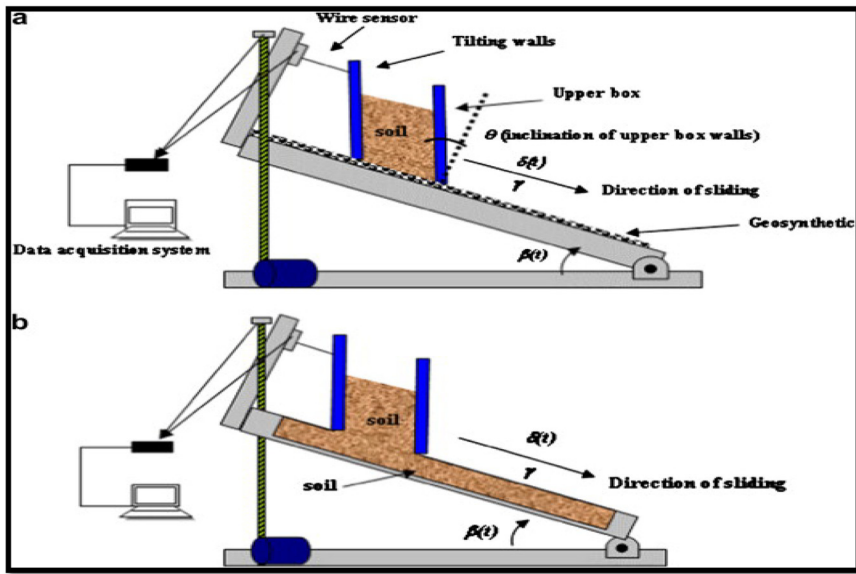


Fig. 2. Tilting box method [35].

with an increase in the amount of the material or the size of the conical heap and tends to increase with slower funnel lifting speeds during the experiment. Moreover, as the base roughness (friction) increases, the angle of repose also increases, and it is nearly impossible to form a heap on a frictionless base. Miura, Maeda and Toki [39] have also developed a reduction factor for the angle of repose as a correction for the pedestal size. However, Shorts and Feitosa [40] have shown that for frictionless grains/bubbles, due to geometrical constraints, the angle of repose may have a non-zero value (in their case, the average angle of repose was found to be 3.75°).

The angle of repose of powders, especially those used in steel casting applications, can be obtained from the funnel method [10,13]. The amount (mass) of the powder is specified in the standard (approximately 454 g), and the tested powder should be homogenous and representative. The height between the base and funnel nozzle is fixed (at approximately 3.81 cm). The powder is then continuously poured from the funnel until the cone of the heap reaches the predetermined height; thereafter, the diameter of the cone is measured. The experiment is repeated twice more. The average diameter is calculated from the three records and rounded to the nearest 25.4 mm (1 in.). Thereafter, the angle of repose is calculated by the (arctan) rule and rounded to the nearest one-tenth of a degree.

Geldart et al. [41] studied the angle of repose of powders to investigate their flowability properties. A modified funnel method was used to measure the angle of repose of a slightly cohesive powder; the results being consistent with the Hausner ratio method. Chukwu and Akande [42] have developed a funnel method to obtain the angle of repose of different agricultural materials for agricultural purposes, such as the design and construction of bins, hoppers and silos. They indicated the importance of both the static and dynamic angles of repose in the field of agriculture. However, Chukwu and Akande [42] measured only the static angle of repose. They used several base types with different roughnesses and various granular materials such as rice and seeds. They reported some differences between their values and the typical values presented in the literature; these differences range from  $\pm 0.96^\circ$  to  $\pm 9.0^\circ$ . The cost to fill the large box was the most significant limitation of the tests.

Nakashima et al. [43] conducted a comparative study between the available data on the angle of repose data of the funnel method in the literature and a 2D DEM simulation for granular soils. They also investigated the effects of gravity, grain size, internal friction angle and rolling friction coefficient, which is the tangent of the rolling friction angle. Nakashima et al. [43] reported that the effects of gravity and grain size were negligible. However, they concluded that a DEM simulation could be used to determine the angle of repose reasonably.

Szalay, Kelemen and Pintye-Hódi [44] proposed that the "cohesion" coefficient is to be related to both frictional and cohesive forces to optimize the funnel size (i.e., minimum/critical orifice diameter) for different sorbitol in capsules and minitablets production process. Further, they have noticed that as the cohesion coefficient increases, the angle of repose linearly increases. As a result, it is suggested to use the angle of repose in the determination of the critical orifice diameter to assure free flowing of the particles.

#### 2.1.3. Revolving cylinder/drum method

The revolving cylinder/drum method is used to determine the dynamic angle of repose, which is usually at least 3 to 10° less than the static angle of repose [45] and is often related to the segregation phenomena of granular materials. Granular materials avalanche when their static angle of repose is exceeded and stop at a dynamic angle of repose [46]. In this method, the granular materials are placed in a cylinder, which has a transparent side. Then, the cylinder is rotated at a fixed speed and while rotating, the materials move and rotate within the cylinder to a maximum angle, which is considered the dynamic

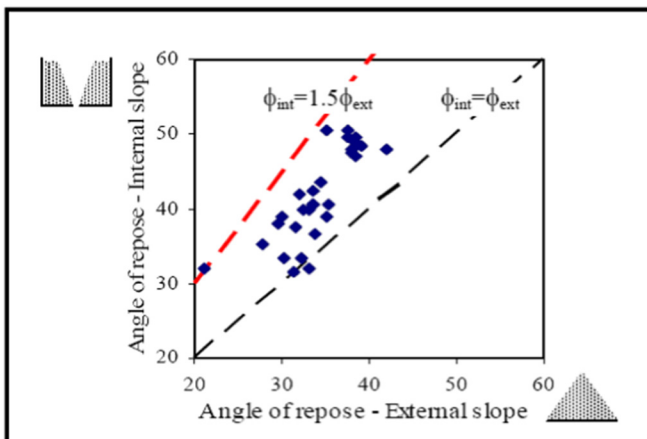


Fig. 3. Comparison between internal and external angle of repose [37].

angle of repose. According to Dury et al. [47], the dynamic angle of repose at the end caps of the revolving cylinder is 5° greater than the dynamic angle of repose elsewhere within the cylinder due to the boundary friction effect. Yang, Zou and Yu [32] noticed a linear increase in the dynamic angle of repose as the rotation speed of the cylinder increases. As the rotation speed increases, the inclined flat surface of the material tends to form an S-shaped surface [48], as shown in Fig. 4.

Liu, Specht and Mellmann [49] measured the dynamic angle of repose for glass beads with different particle and drum sizes and suggested that the dynamic angle of repose is approximately equal to the average of the upper and lower dynamic angles of repose in a rotating drum [50]. The upper dynamic angle of repose is the angle at which the granular material at the drum bed starts to avalanche, while the lower angle is the angle at which the granular material rests when the avalanche stops. The upper and lower dynamic angles of repose were assumed to be independent of each other; however, Liu, Specht and Mellmann [49] found a linear correlation between the upper and lower dynamic angles of repose. They have compared this proposed linear correlation with 14 types of materials (glass beads, fertilizer pellets, steel balls, steel cylinders, steel scraps, activated carbon, wood, grit, gravel, foam clay, fertilizer fragments, etc.) with particle sizes ranging from 0.35 to 15 mm. The results of the measured and predicted dynamic angles of repose matched well. Therefore, only one angle (e.g., the upper dynamic angle of repose) must be obtained to calculate the lower dynamic angle of repose and, subsequently, the dynamic angle of repose. Moreover, they noticed that the dynamic angle of repose increased when the ratio of the particle size to drum size increased, while the rotation speed and filling degree had marginal effects on the test results. Nevertheless, it was noted that the filling degree and Froude number is do affect the dynamic angle of repose as well as the peak velocity of the particles in a rotating drum [51].

#### 2.1.4. Hollow cylinder method

The hollow cylinder method is employed to determine the static angle of repose of a cohesionless material. The test material is placed into a hollow cylinder of a certain diameter and height atop a selected base with known roughness properties. The cylinder is then carefully pulled off of the base, like in a concrete slump test, at a particular velocity to allow the material to flow and form a conical shape [52]. The angle of repose is then measured by the (arctan) rule.

Lajeunesse, Mangeney-Castelnau and Villette [53] investigated the flow dynamics of granular materials by measuring the angle of repose for slope stability applications. The authors used glass beads with two different sets of grain sizes. They qualitatively examined the effects of the bead grain size and base roughness on the angle of repose as well as the influence of the base rigidity and granular material mass. Lajeunesse, Mangeney-Castelnau and Villette [53] used the hollow cylinder method with different sizes at a constant lifting velocity (approximately 1.6 m/s). The test methodology was well controlled, and they used a fast camera (500 images/s) to record the experiments, as shown in Fig. 5. They thoroughly discussed the experiment instrumentation, energy dissipation and deposit morphology. However, they reported that the aspect ratio of the initial height of the granular material to the radius of the cylinder has the most significant effect on the angle of repose.

Liu [7] extended the above-mentioned work [53] and determined the angle of repose for civil engineering applications, mainly for slope stability, by using the hollow cylinder method. He quantitatively investigated the effects of the stratification, interface friction angle (which is the friction angle between the base and the granular material), lifting velocity, cylinder size, base roughness, granular material mass and height of the sand in the cylinder. Many correlations have been developed by considering these factors. He also found that the angle of repose and the internal friction angle were approximately equal. Liu [7] concluded that as the lifting velocity, material mass and material height increase, the angle of repose decreases. However, when the roughness of the base increases, the angle of repose also increases. For sand-gravel mixtures, the contribution of the sand to the angle of repose was minimal compared to that of pure sand. Similar studies have utilized this method to determine the static angle of repose [54–58].

#### 2.1.5. Tilting cylinder method

Another method has been proposed to measure the angle of repose of granular soils [6]. In the tilting cylinder method, the soil is poured vertically into a water-filled graduated cylinder, and then the cylinder is tilted >60° slightly and slowly restored to its vertical position. Then, the angle of repose is considered the slope angle of the residual soil within the cylinder. Using this method; a linear correlation between the roundness of the particles and the angle of repose has been proposed, as shown in Fig. 6. However, different definitions and methods have been used to determine the roundness of the particles, as will be discussed later, and the type of correlation should be utilized with extreme caution.

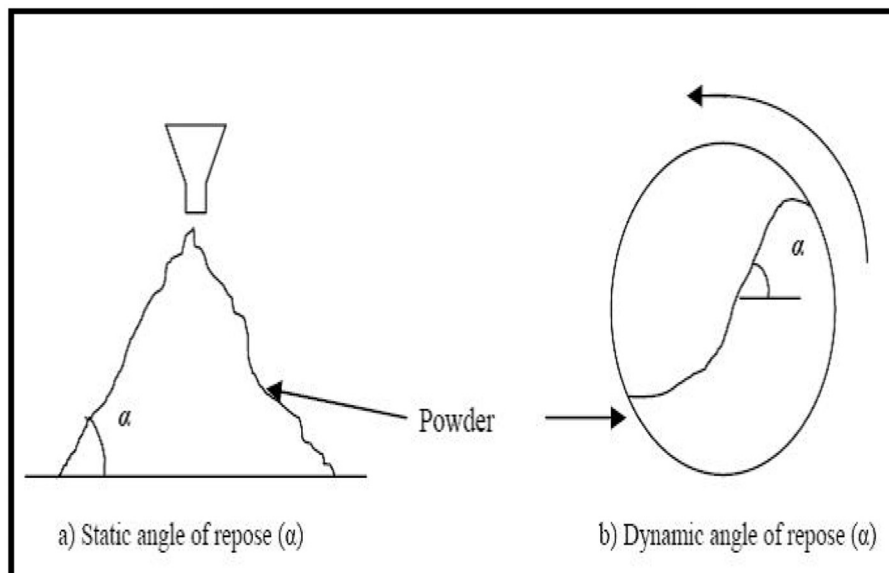
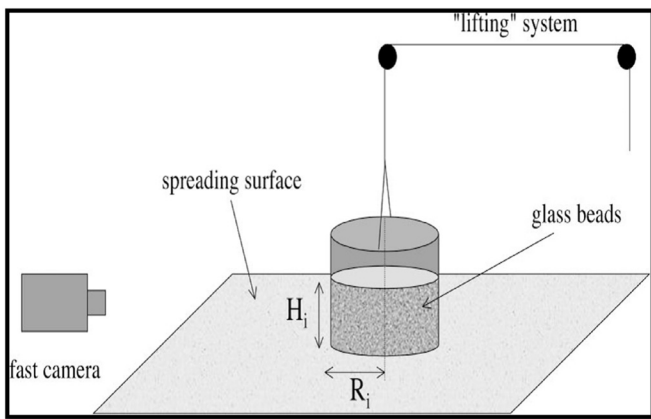


Fig. 4. (a) Static angle of repose (b) S-shaped surface in dynamic angle of repose measurement [48].



**Fig. 5.** Controlled hollow cylinder test [53].

#### 2.1.6. Comparison

Rousé [50] compared six methods for measuring the angle of repose of six types of granular soil. She indicated that the highest value of the angle of repose was obtained from the ASTM International method [7]. The differences between the six methods led to a difference in the factor of safety of approximately 82% for slope stability applications with considerable differences in the soils that require excavation. Therefore, drawing a conclusion or conducting a comparison between the different methods of measurement may be challenging because each measurement method is targeted for a specific application. For instance, it may be inappropriate to design a silo with the angle of repose obtained from the rotating drum method. The tilting box method is used based on the assumption that the angle of repose and friction angle are equal, which is not always accurate [21]. The funnel method is widely used in silo design, pharmacology, and bulk material handling. However, the funnel method may be recommended in the cases where the granular particles are jammed or undergo jamming transition. Jamming is a new phase transition that was formerly known as glass transition [59]; the particles jam if either the density is increased or the temperature is lowered, which can considerably slow the dynamics of the particles until the material becomes rigid, similar to the bottleneck phenomenon in a traffic jam. In silos, jamming occurs due to the arch formation of the particles at or near the outlet of the silo; hence, a critical/minimum outlet size should be selected to prevent or reduce jamming [60]. Alternatively, jamming can be reduced by vibrating the silo to prevent the outlet from clogging [61]. It has recently been reported in the news that a collapse of a corn silo of 10,000 tons in Ohio, USA, affected the power lines and poles and shut down the Ohio road for days,

while the investigations are still ongoing [Associated Press (2018, January 22). Silo collapse sends about 10,000 tons of corn onto road. The Washington Post. Retrieved from <https://www.washingtonpost.com>]. However, the angle of repose might be found to have a significant role in the study.

The revolving drum method is used when the dynamic angle of repose is of concern to investigate, for example, the segregation and dustiness of the particles to optimize the manufacturing of bulk materials. The hollow or bottomless cylinder method is primarily used to study the effect of reducing or removing the confinement pressure on a slope or a pile of granular materials under disturbance or dynamic loading. While the tilting cylinder method; can be used to study the formation of sediment dunes, for instance, on the seabed or in oceanic trenches.

#### 2.2. State-of-the-art methods

As noted above, even within the same method of measurement, considerable variation and issues may occur regarding the repeatability (i.e., the error between two measurements performed by one operator under the same conditions) and reproducibility (i.e., the error between two measurements performed by different operators in different laboratories under the same conditions). For this purpose, an interlaboratory experimental study was conducted to measure the angle of repose according to the ASTM standard method [7]. Five different laboratories participated in this study; each of the laboratories employed two operators to measure the angle of repose of a mold powder, and each operator repeated the measurement three times. As a result, the maximum repeatability of the 95% confidence interval was within 1.4°, while the maximum reproducibility of the 95% confidence interval was 2.4°. Such a vast difference between the measurements, among other reasons, led to the withdrawal of the ASTM method. Therefore, a global, state-of-the-art standardized method is needed.

Furthermore, the angle of repose of two piles of granular material can be compared only if the piles have even, regular slopes, which are not exhibited for cohesive material or extremely angular particles. All the previously discussed methods of measurement assume that the granular material piles form perfect conical shapes, unlikely the case for the majority of other materials. Fraczek, Złobiecki and Zemanek [62] measured the angle of repose for different agricultural materials under various moisture contents using the fixed funnel method. They proved that most of the tested materials exhibited deviations from the assumed conical shape with either truncation of the upper part of the pile, convexity of the slope, or concavity of the slope. The authors used digital image analysis techniques to analyze and obtain the coordinates of a surface profile of the pile slope, and a similar method was reported by Rackl and Hanley [63]. Subsequently, the surface profile was plotted and linearly approximated by using the least squares method, which can reduce the errors in the traditional direct measurements and increase the accuracy in the angle of repose values. In addition, they calculated the required statistical repetitions of the measurements for both the traditional and image-based methods and found out that the maximum number of repetitions needed for the image-based method is approximately 50% less than the maximum number of repetitions required for the conventional method (direct measurement by ruler and protractor or by using the height and diameter in the arctan method). Additionally, Rackl et al. [31] presented similar observations for the heap deviations from the ideal conical shape. They conducted 108 runs to measure the angle of repose of 8 different granular materials using an automated hollow cylinder instrument with various sizes and lifting velocities. The granular materials were heaped onto a rotating plate, and the piles were scanned using 3D scanners. Rackl et al. [31] found that the cohesion, segregation of the particles due to the broad grain size distribution, and non-sphericity of the particles contribute to the deviations from the ideal conical shape. They recommended

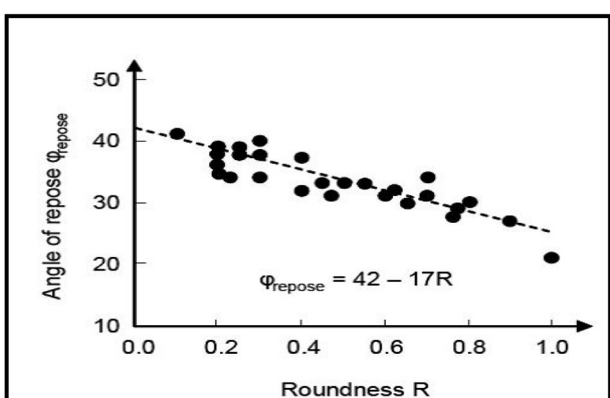


**Fig. 6.** Effect of roundness on the angle of repose [19].

that for consistent measurement of the angle of repose for the required sample volume, the ratio of the heap diameter to the particle size should exceed 40 instead of 20, which was stated in the European Federation of Materials Handling (FEM) standard [64]. However, research and development to enhance the precision and reliability of the angle of repose measurements are ongoing [65–67].

### 3. Applications of the angle of repose

The angle of repose has been utilized in many applications including the transportation and storage of goods, aeolian formations, slope stability, avalanches, barchan dune formation, concrete slump testing, bulk cargo, mass wasting, oceanic trench, retaining walls, sand volcanoes, scree, rotary kiln, mountaineering, simulation model calibration, pharmacology, physics, geology, agricultural engineering, mining engineering, and geotechnical engineering. The angle of repose belongs to a relatively contemporary field of study, and further investigation is needed to broaden the limited information available in this field.

#### 3.1. Major applications

##### 3.1.1. Agricultural engineering

The angle of repose is widely used in the field of agriculture in the design and dimensioning of silos, tanks, hoppers and bunkers to determine the capacity and required volume of the stored and transported seeds, wheat, rice, flour, etc. In the literature, several studies have provided a range of angles of repose for different agricultural materials. For instance, Zaalouk and Zabady [68] have investigated the effects of wheat moisture content and base roughness on the angle of repose for agricultural purposes. The authors developed linear correlations between the angle of repose and moisture content for each set of samples, as shown in Fig. 7, considering the effects of the base roughness. They reported correlation coefficients ranging from 0.77 to 0.99.

##### 3.1.2. Entomology

Botz et al. [69] have studied sand pits constructed by antlions, as shown in Fig. 8. They measured the angle of repose of sand samples using the revolving cylinder method and measured the angle of repose of the antlion pits with laser technology. They also performed comprehensive physical, observational, chemical and statistical analyses. The antlions pits were built at inclination angles that were not significantly different from the angle of repose. The stability of the antlions walking on the slope was also discussed. It was noted that larger antlions were more likely to roll down the slope.

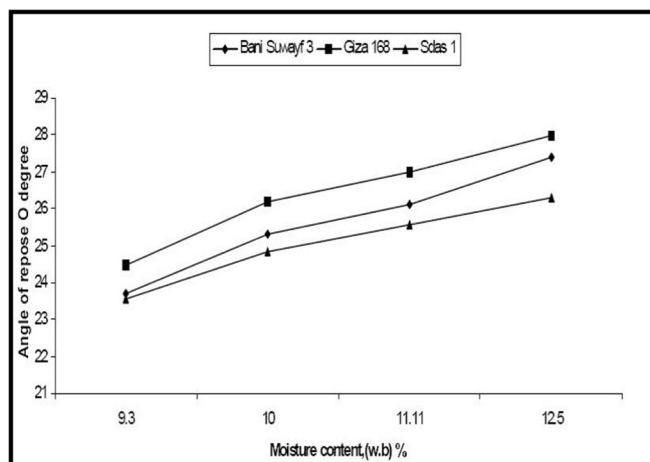


Fig. 7. Effect of moisture content on the angle of repose of different wheat types [68].

#### 3.1.3. Geotechnical engineering

The geotechnical applications of the angle of repose are nearly endless. In this field, the utilization of the angle of repose and the determination of its relation to other engineering properties are still being studied. The appeal of the angle of repose is shown in slope stability problems whereby the slope of the soil or granular geomaterial becomes unstable when its slope angle exceeds the angle of repose, as shown in Fig. 9. In contrast, when a slope experiences toe-cutting or slope modification to an angle that exceeds the angle of repose, flow deposits will slide downslope to recover a stable slope angle, i.e., the angle of repose, as shown in Fig. 10. For example, the phenomena of rockfall and mass wasting, as shown in Fig. 11, occur to recover a stable slope angle. In addition, the angle of repose can be utilized in the design of barriers or rockfall collectors. Moreover, in certain cases such as backfilling, if the slope angle of the soil exceeds the angle of repose, a retaining structure will be required to maintain the slope stability. Therefore, the angle of repose of the soil can simply be used to justify whether a retaining wall or structure is needed, as shown in Fig. 12.

Metcalf [21] investigated the relationship between the internal friction angle and the angle of repose of crushed rocks on the basis of physical experiments. He concluded that the angle of repose, in general, is not equal to the angle of internal friction of the heaped material but is the angle of internal friction for the same material under its loosest condition. Evesque and Rajchenbach [70] investigated the factors that affect the slope stability of a heap of granular materials subjected to a low-frequency vertical vibration and a sufficiently large amplitude. They concluded that the stability of the slope is governed by the angle of repose, amplitude of the vibration, convective transport within the material itself and acceleration of the vibrations. Lee and Herrmann [71] studied the angle of repose of a finite slope of granular materials using a 2D molecular dynamics simulation. However, they defined the angle of marginal stability, which is the maximum stable angle of a heap but it is not necessarily the angle of repose, as they declared. Static friction has been studied much less than the other microscopic phenomena, mainly due to the difficulty of generating a theoretical formulation or simulation models for the static friction. Lee and Herrmann [71] found that the angle of marginal stability is larger than the angle of repose and developed a theoretical expression for the angle of marginal stability by assuming a particular stress distribution. They considered spherical, homogeneous sand particles in their model and incorporated favorable physical properties and assumptions. Of the studied parameters, the angle of repose was markedly affected by only the angle of internal friction between the particles. Additionally, they comprehensively discussed their models and theoretical assumptions; although they calculated and measured both the angle of repose and angle of marginal stability, they considered their work a qualitative study due to these assumptions and limitations. However, for large-scale granular materials, the final slope was found to rest at an angle lower than the angle of repose [72].

Chik and Vallejo [73] measured the angle of repose for coarse and fine sand mixtures on rough and smooth bases. The authors developed theoretical relationships between the angle of repose, the internal friction angle of the mixture and the angle of interface friction. Ghazavi, Hosseini and Mollanouri [74] introduced a modified funnel method to measure the angle of repose of sand. Three types of sand samples were tested in their angle of repose experiments and angle of internal friction simple shear box tests, at the same compaction densities. For each sand, a linear correlation was generated between the angle of repose and the internal friction angle with a high correlation coefficient of 0.96. However, the correlations between the angles of repose and internal friction angles are valid under very restricted conditions, as highlighted earlier.

#### 3.1.4. Hydrodynamics and sedimentology

The flow and heaping of sediments on the beds of streams, rivers and dams, as well as in oceanic trench slopes, are closely related to the angle

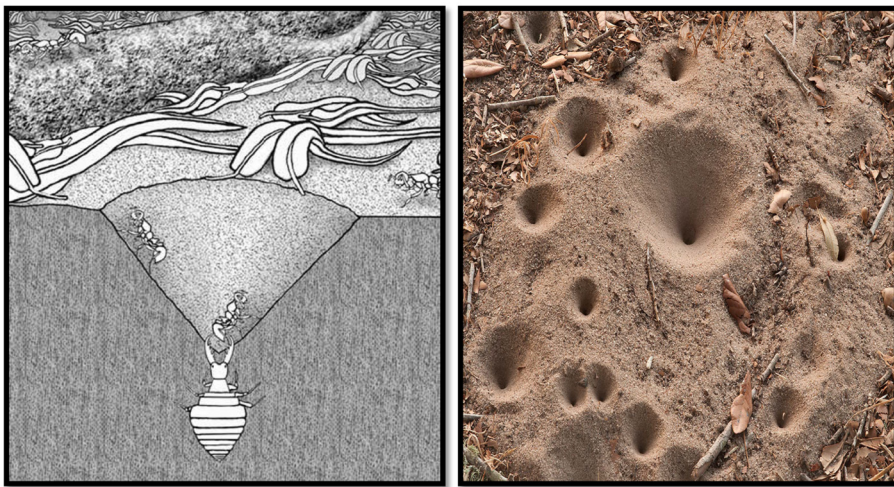


**Fig. 8.** Angle of repose of an antlions pit ([www.bugs.bio.usyd.edu.au](http://www.bugs.bio.usyd.edu.au)).

of repose of the sediment material, such as sand, silt and clay. The angle of repose of sediments was theoretically [75,76] and experimentally [77] examined. Yang et al. [78] investigated the angle of repose of non-uniform sediments to study bed slopes and sediment transportation. The angle of repose of the sediments was tested by using air and water in a method similar to the revolving cylinder method. The effects of the rotation velocity, filling degree and weight ratio of the sediments on the angle of repose were investigated. An empirical equation was generated to predict the angle of repose; this equation was tested for a broad range of laboratory data on the angle of repose and found to be reasonably acceptable. A thorough study of the formation of dunes underwater has recently been reported by Kwoll et al. [79].

### 3.1.5. Particle technology and materials science

The flowability of granular material is usually linked to the angle of repose, as discussed earlier. The concrete slump test can directly determine the angle of repose in a way similar to the hollow cylinder method. Material segregation studies, especially for steel and aggregate mills and cement kilns [80], is another method to directly determine the dynamic angle of repose in a way similar to the revolving cylinder method. In a recent study using glass and polypropylene beads [81], it was proven that the segregation index is decreasing when the dynamic angle of repose increases.

Riley and Mann [82] investigated the angle of repose and the Hausner ratio for different glass particle shapes, similar to the work of Lajeunesse, Mangeney-Castelnau and Vilotte [53]. Both spherical and non-spherical glass particles, in addition to a mixture of particle shapes, were tested. The relationship between the angle of repose and the Hausner ratio is unpredictable. Riley and Mann [82] recommended using the Hausner ratio as a general index for the frictional properties due to its simple measurement approach.

Zhou et al. [83] studied the angle of repose of coarse spherical glass bead particles numerically by using the modified DEM and experimentally using the internal funnel method. From their model, they developed an empirical formula for the angle of repose for engineering applications and validated it with the results of their experiments. They declared that the angle of repose is affected by the rolling friction of the particles, container thickness and particle size, while it is not affected by damping, Poisson's ratio, Young's modulus or the restitution coefficient. They also generated a predictive formula for the initial angle of repose from the particle size and then employed this formula in a correction equation to obtain the angle of repose with a maximum error of estimation of 3.0°. However, when the angle of repose is small, a large relative error is expected. The predictive formula is applicable for the material conditions tested by Zhou et al. [83] to determine the angle of repose, as shown in Eq. (1). The static angle of repose is

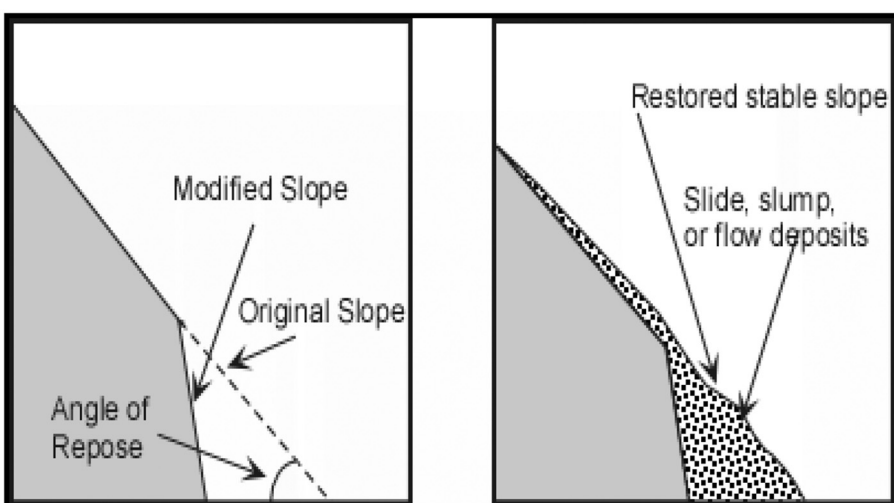


**Fig. 9.** Role of the angle of repose in slope stability ([www.personal.kent.edu](http://www.personal.kent.edu)).

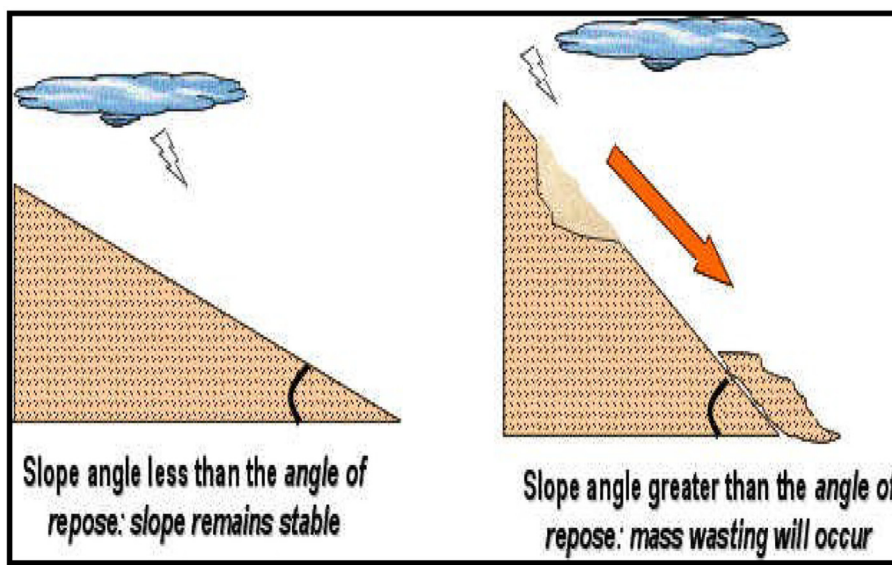


**Fig. 10.** Recovered stable slope ([www.tulane.edu](http://www.tulane.edu)).

positively correlated with the sliding and rolling friction coefficients of particle-particle and particle-wall cases, while, it is negatively correlated with the particle size, as reported elsewhere throughout the literature. However, it is to be noted that their equation is valid for the provided range of the parameters, measurement method and the tested material, and further enhancements of the fitting parameters in the equations are required to cover a broader range of particle sizes and types.

Angle of repose estimation from DEM simulation [83]:

$$AOR = 68.61 \times \mu_{S,PP}^{0.27} \times \mu_{S,PW}^{0.22} \times \mu_{R,PP}^{0.06} \times \mu_{R,PW}^{0.12} \times d^{-0.2} \dots \quad (1)$$

where:  $AOR$  = angle of repose, degrees;  $\mu_{S, PP}$  = sliding or static friction coefficient (particle-particle), 0–0.6;  $\mu_{S, PW}$  = sliding or static friction coefficient (particle-wall), 0–0.6;  $\mu_{R, PP}$  = rolling friction coefficient (particle-particle), 0–0.1 mm;  $\mu_{R, PW}$  = rolling friction coefficient (particle-wall), 0–0.2 mm; and  $d$  = particle diameter, 2–10 mm.

Li et al. [84] studied the static angle of repose of iron ore particles experimentally (using a funnel method), and numerically through DEM simulation. They have provided highly positive linear relationships between the angle of repose and sliding and rolling friction coefficients, and a profoundly negative linear relationship with the mean particle size.

### 3.2. Other applications

The above review indicates that the angle of repose could be utilized in different applications and for various purposes. The angle of repose can also be used by mountaineers to determine the slopes that are safe for their activities. In geology, the angle of repose is used to illustrate and predict the steepest slope of barchan dunes, which are crescent-shaped sand dunes [85], as shown in Fig. 16. Sand boils, or sand volcanoes, are conically shaped and form when sand is ejected onto the surface from a weak central point; these features are sloped by the angle of repose of the sand. Further, sand volcanoes are related to the soil liquefaction phenomenon that occurs during earthquakes [86]. In the transportation and storage of goods such as coffee bins, coconuts, seeds, and tires, the angle of repose is used in the design of containers and tanks to determine their necessary capacity and height [68].

In pharmacology, the angle of repose is used to indicate the flowability of granular powders used in drug production and coating [87,88]. Train [89] measured the angle of repose using different methods (tilting box, fixed and lifted funnel and revolving cylinder methods) for different powders, including silver sand. From his measurements, the angle of repose of the silver sand ranged from 31° to 34°, as shown in Fig. 17. He suggested that if any method is used to determine the angle of repose, the practical conditions should be rigidly defined to obtain comparable data.

The angle of repose is used not only for terrestrial applications but also extraterrestrial applications. Granular materials avalanche when their slope exceeds the static angle of repose and stop at the dynamic angle of repose; these phenomena were assumed to occur independently of gravity. However, Kleinhans et al. [46] investigated the effects of reduced gravity on the dynamic and static angles of repose to demonstrate the avalanche behavior of granular material on Mars and asteroids. They used revolving cylindrical instruments housed in an accurately controlled airplane and conducted 33 parabolic flights under effective gravities of 1.0, 0.38 (Mars) and 0.1 times the terrestrial gravity, as shown in Fig. 18. Different particle sizes and shapes have been studied in either water or air, which were used as lubricant fluids. In general, the static angle of repose increased by 5° with the reduced gravity, while the dynamic angle of repose decreased by 10°; consequently, the avalanche size increased. Therefore, the authors suggested that, on Mars, the granular materials at relatively low slopes might have formed in dry conditions without lubricating fluids. Kleinhans et al. [46] proved that the angle of repose is a gravity-

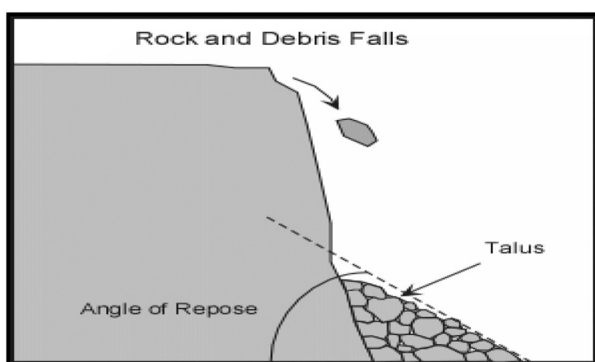


**Fig. 11.** Illustration of mass wasting and rockfall due to exceeding the angle of repose ([www.tulane.edu](http://www.tulane.edu)).

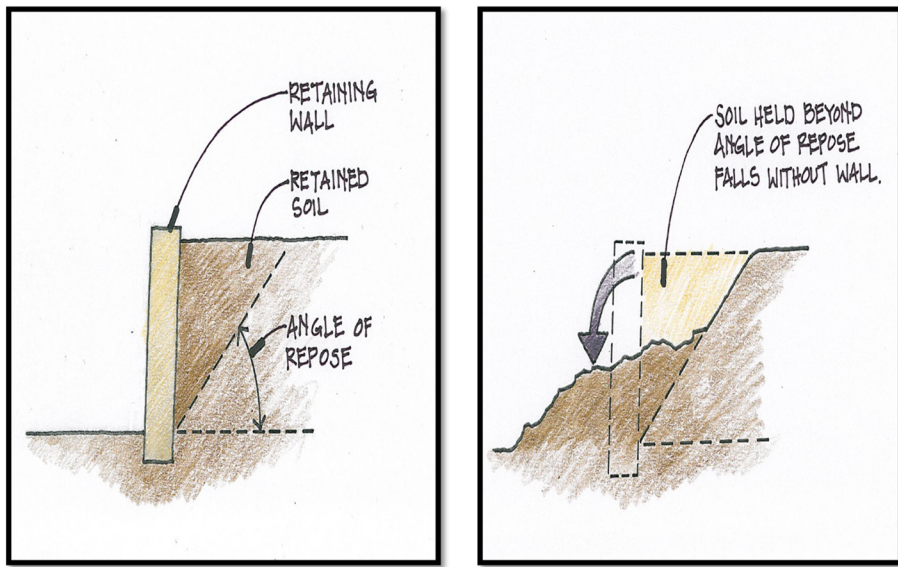


**Fig. 12.** Retaining wall justification by using the angle of repose ([www.patio-supply.com](http://www.patio-supply.com)).

dependent parameter, but further research, considering all other possible factors, is recommended.

Remote sensing technology and geographical information system (GIS) analyses have allowed scientists to measure the dynamic angle of repose of real Martian sand dunes and compare the results with those of terrestrial sand dunes [90]. It has been found that both the Martian and terrestrial sand dunes have similar dynamic angles of repose, implying that this angle is independent of gravity; however, this result diverges from the results of the experiments of Kleinhans et al. [46].

In mining activities, such as mineral piling or mining drilling, the angle of repose is considered an essential factor in the design of the collection area and drilling slopes. Hancock et al. [91] monitored and simulated the rills that form slopes at the angle of repose. They used laser technology and the SIBERIA erosion model to simulate rill formation in mining sites and agricultural fields whereby a single rainfall or runoff event can create new rills that affect those sites. The SIBERIA erosion model was able to determine the behavior of rills in both time and space from adequate input parameters, one of which is the angle of repose.

### 3.3. Calibration of numerical models and simulations

Granular material is a discrete material and, unlike continuous material, is more complex to simulate. To obtain realistic results from numerical simulations of natural and real materials, the input parameters and particle properties must be accurate. The challenges in numerical simulation arise due to the difficulty in experimentally determining the particle properties, such as rolling friction, restitution coefficient, inter-particle friction, particle shape and size, particle density, dilation angle and particle stiffness. Therefore, the use of a calibration method has been proposed to calibrate and ensure the simulation results [92]. Two types of calibration are used. In direct calibration, the simulation is calibrated by experimentally measuring the particle properties and then using them as the simulation inputs. In indirect calibration or reverse calibration, a bulk property is measured, such as the distribution of particle size, bulk (packing) density and angle of repose [93], and then a set of simulation parameters is changed until the measured bulk properties are matched. A calibration method is used to simulate and optimize the handling process of bulk solids.

Wangchai, Hastie and Wypych [94] used a DEM to simulate a revolving cylinder dustiness test to monitor and quantify dust generation in mining activities to minimize dust generation and its impact on the environment. The authors used a non-dusty material, namely polyethylene pellets, to calibrate the DEM before being used to simulate dusty materials. They determined the restitution coefficient, which is the ratio of the rebound height to the initial height of the particle before the impact, as well as the particle density, particle size and shape, angle of repose, and friction coefficients between the particles and cylinder walls. The static and rolling friction coefficients of the particles estimated from the model were approximately the same as the measured properties. Wangchai, Hastie and Wypych [94] also modeled different particle shapes using single and multiple spheres, as shown in Fig. 13. The effects of the various particle shapes on the static and rolling friction coefficients were determined from a sensitivity analysis of the angle of repose, conducted by using the DEM simulation, as shown in Fig. 14. The heap or pile of different particle shapes was simulated in the DEM. When the rolling friction coefficient of the particle was 0.2 and the static friction coefficient of the particle was 0.1, the simulated results matched closely with the experimental results, as shown in Fig. 15. The authors concluded that DEM could be utilized to obtain accurate results for granular materials. Finally, they suggested coupling the DEM with computational fluid dynamics (CFD) to model the air flow around the particles. However, many published studies suggest the usage of a reverse calibration method by physically measuring the bulk properties (e.g., the angle of repose) and then adjusting the DEM simulation properties to match the measured properties [95–103].

Brezzetti et al. [104] used the hollow cylinder method to calibrate a material point method (MPM) simulation. MPM is a meshless numerical simulation method used to obtain results that are independent of the mesh size, shape or condition. The authors aimed to determine the rheological parameters of a Bingham model by run-out simulation. A mixture of water, sand and kaolin was used in the physical experiment, and the height and diameter of the mixture in the hollow cylinder were recorded using a high-speed camera while lifting the cylinder to correlate the height and diameter with the run period. Brezzetti et al. [104] noticed that when the kaolin content in the mixture increased, the height of the pile increased, while the diameter decreased (i.e., the angle of repose increased). Moreover, a number of other studies that utilized the angle of repose, especially in a DEM, have been reported [92]. The ability of DEM

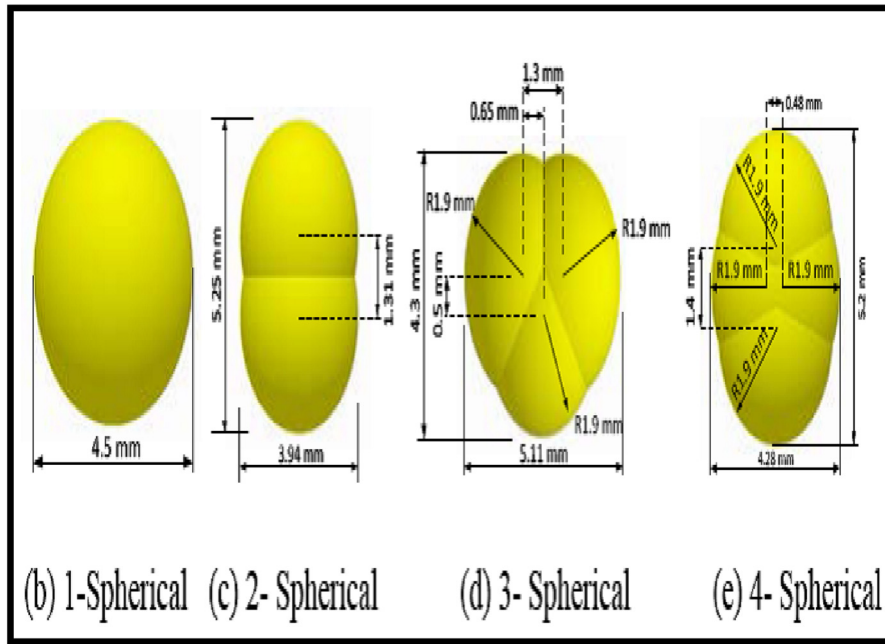


Fig. 13. Particle shape simulation in a DEM [94].

simulations to predict the contact and inter-particle parameters has been proven, especially when the exact shape of the particles are simulated using other methods such as multiple spheres; in this case, DEM simulations can be used instead of the complicated physical measurements [105,106]. A comparative study between the DEM and MPM was recently conducted by Kumar et al. [107], who have demonstrated the ability of the MPM to simulate the granular flow dynamics with a single input parameter: the internal friction angle. The authors reported good agreement between the DEM and MPM methods.

#### 4. Influential factors

Some of the particle and inter-particle properties of granular materials can be calibrated using the numerical simulations with the angle of repose of the bulk material; therefore, such properties (i.e., factors

influence the angle of repose. Accordingly, knowledge of these factors is important and; hence, a review of the most influential factors is presented below.

##### 4.1. Geometrical properties of the particles

As discussed earlier, the particle shape and size significantly affect the angle of repose values. For instance, the effect of roundness of soil particles on the angle of repose is shown in Fig. 6. Additionally, shape descriptors are scale-dependent factors [6]. Further, the scales at which the particle shape is described are as follows: the global form, the scale of the surface roughness and the scale of the major surface features [19]. At these scales, the following factors and properties are known as shape descriptors: particle roundness, sphericity, roughness, size, aspect ratio, slenderness, solidity, Ferret diameter, irregularity,

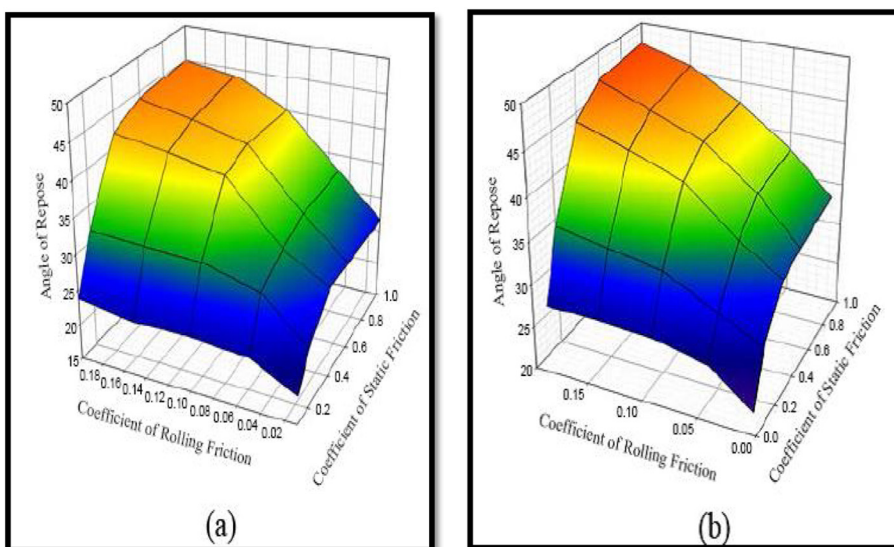
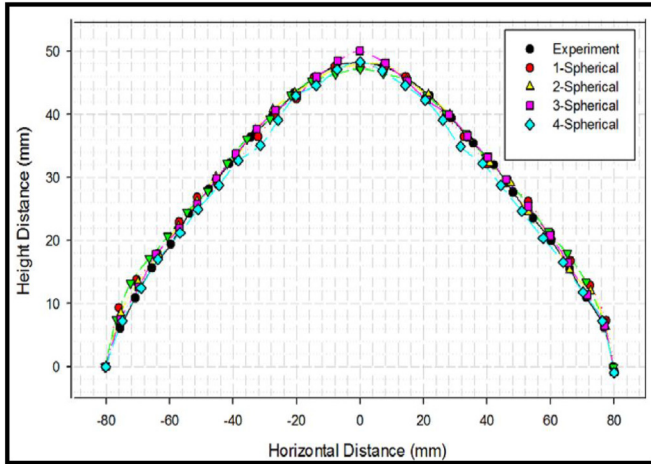
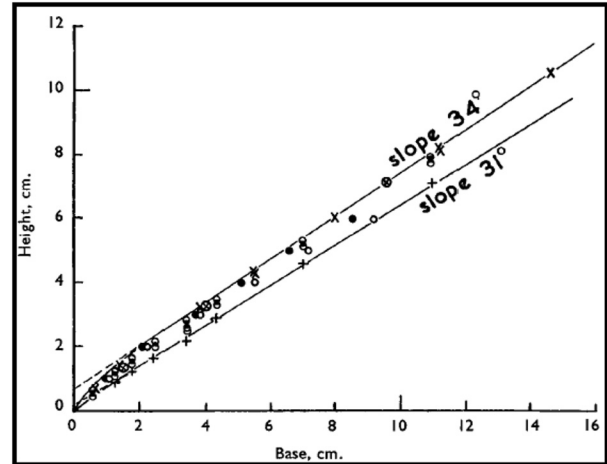


Fig. 14. Effect of rolling and static friction coefficients on the angle of repose (a) Single sphere particles and (b) Double spheres particles [94].



**Fig. 15.** Comparison between slump tests and DEM simulations [94].



**Fig. 17.** Angle of repose range of silver sand [89].

elongation, fractal dimension, etc. According to Ulusoy, Yekeler and Hıçyılmaz [108], no shape descriptors are universally accepted or standardized; nonetheless, the effects of the shape descriptor are described below.

#### 4.1.1. Particle roundness

There are different definitions available in the literature for 2D and 3D particle roundness. Relations between the roundness and the angle of repose, or any other factor, should be considered in the context of the “defined” roundness and the method used to determine the angle of repose. The roundness is highly dependent upon the sharpness of the particles and is usually related to their angularity. The most commonly used definition of the roundness of a particle was proposed by Wadell [109], who defined it as the ratio of the average curvature radius of the particle edges and corners to the radius of the maximum inscribed sphere. From this definition, Krumbein and Sloss [110] developed the so-called roundness and sphericity chart for visually determining roundness, as shown in Fig. 19. With the Wadell roundness [109], Powers [111] provided a shape classification based on the roundness, as shown in Table 3. Mitchell and Soga [6] reported two other definitions of roundness, as presented below in Eq. (2) and Eq. (3). Li et al. [112] discussed the Cox roundness, also known as circularity, and defined it from the projected area and projection perimeter of the particle, as shown in Eq. (4).

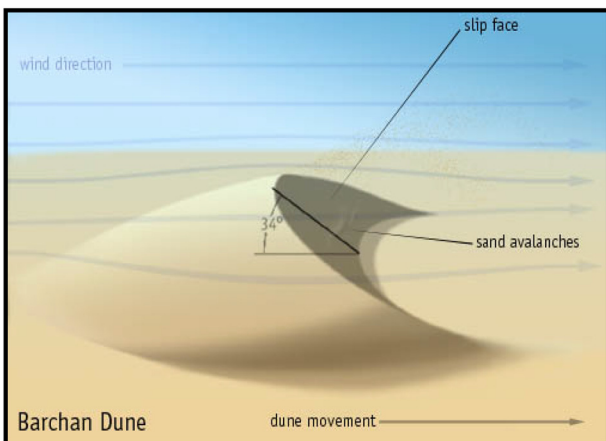


**Fig. 16.** Angle of repose of barchan dunes (Wiki).

Roundness 2 [6]:

$$R_2 = \frac{2 \times d_C}{D_L} \dots \quad (2)$$

Roundness 3 [6]:

$$R_3 = \frac{d_C}{D_{av}} \dots \quad (3)$$

Cox roundness or circularity [112]:

$$R_{Cox} = \frac{4\pi \times A_{PR}}{(P)^2} \dots \quad (4)$$

where:  $R_2$  &  $R_3$  = roundness types 2 and 3, respectively, as defined by Mitchell and Soga [6];  $d_C$  = curvature radius of the maximum convex part of the particle;  $D_L$  = longest diameter through the most convex part of the particle;  $D_{av}$  = mean radius;  $R_{cox}$  = roundness or circularity [112];  $A_{PR}$  = particle projected area; and  $P$  = overall projection perimeter.

A visual determination of the roundness of granular material, such as soil, is not always applicable; instead, different techniques are



**Fig. 18.** Revolving cylinders housed in an airplane to measure the angle of repose under low gravity [46].

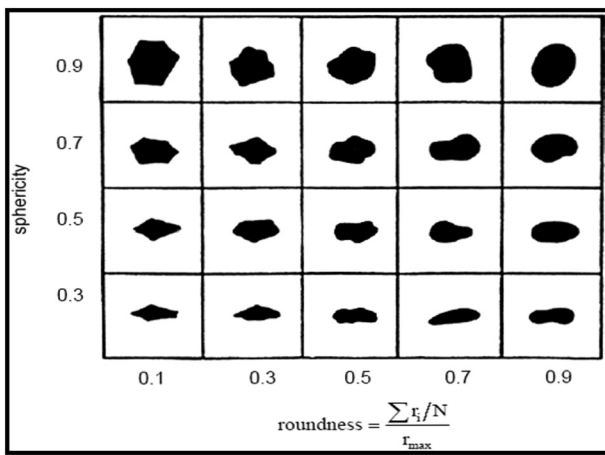


Fig. 19. Roundness-sphericity chart [110].

often used, such as fractal analysis, Fourier methods and image analysis and processing [6]. Santamarina and Cho [19] studied the effect of particle shape of coarse- and fine-grained soils on their fabric and macroproperties, such as fabric anisotropy, density, void ratio, oedometric stiffness, strength, critical state friction angle, drained and undrained shear strength, and liquefaction. They used the Wadell criteria [109] to define the particle roundness. They noted that when the uniformity coefficient of the sand ( $C_u$ ) = 1.0 and the roundness or sphericity of the sand increased, the minimum and maximum void ratios decreased, as reported in Eq. (5) by Youd [113]. The uniformity coefficient ( $C_u$ ) is a measure of gradation for the grain size distribution [114] and determined as the ratio of ( $D_{60}/D_{10}$ ); where  $D_{xx}$  is the

corresponding particle size at which XX% of the particles are smaller. An increase in  $C_u$  led to a decrease in both maximum and minimum void ratios [113]. Additionally, they noticed a negative linear relationship between the angle of repose and the Wadell roundness [109], as shown in Fig. 6. They recommended that a determination of the shape descriptors be conducted for each soil characterization.

Roundness effects on minimum and maximum void ratios for sand at  $C_u = 1.0$  [113]:

$$e_{\max} = 0.554 + \frac{0.154}{R}, e_{\min} = 0.359 + \frac{0.082}{R} \dots \quad (5)$$

where:  $e_{\max}$ ,  $e_{\min}$  = maximum and minimum void ratios, respectively; and  $R$  = Wadell roundness [109].

Cheshomi, Fakher and Jones [115] studied the peak friction angle of sand in coarse alluvial deposits; this angle being often determined by the so-called shear box test and the particle roundness and sphericity. The peak friction angle increased when the roundness decreased or the sphericity increased, as shown in Eq. (6). The authors used this equation to obtain a correlation coefficient of 0.86 from their results.

Relationship between peak friction angle, roundness and sphericity [115]:

$$\phi_p = 19.9 + \frac{10.6 \times S}{R} \dots \quad (6)$$

where:  $\phi_p$  = Peak friction angle determined from shear box test, degrees;  $R$  = Wadell roundness [109]; and  $S$  = Wadell volume-based sphericity [109].

Zheng and Hryciw [116] proposed a numerical computational geometry method that uses images to determine the soil roundness, roughness and sphericity. They computed the mean surface by conducting a locally-weighted regression analysis validated by K-fold

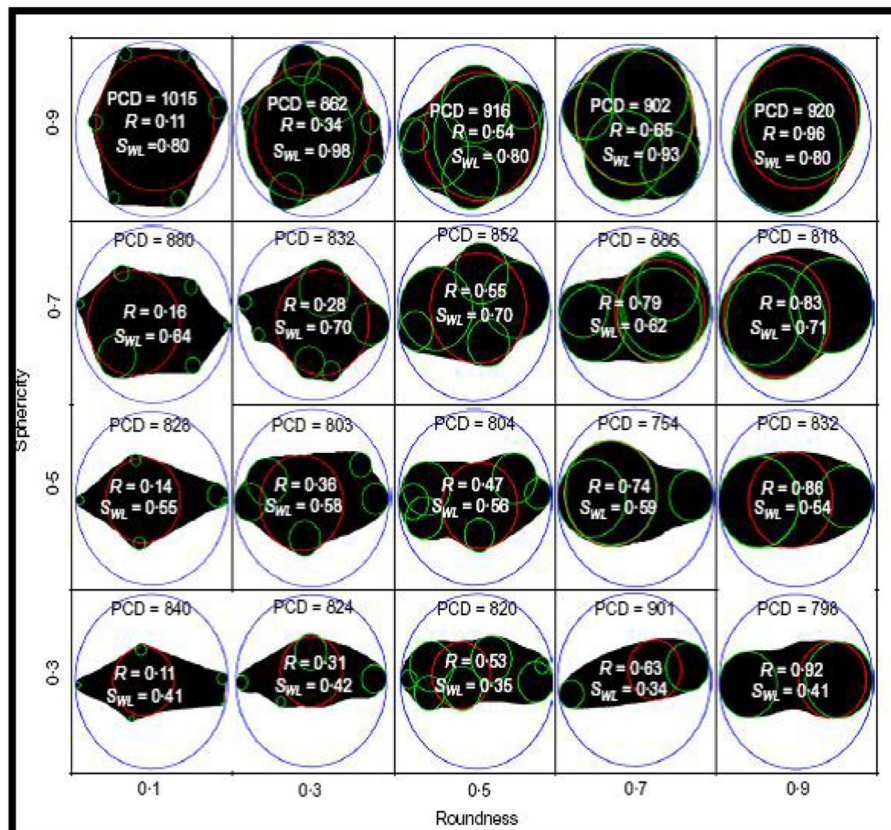


Fig. 20. Comparison between methods (Krumbein and Sloss 1963; Zheng and Hryciw 2015) [116].

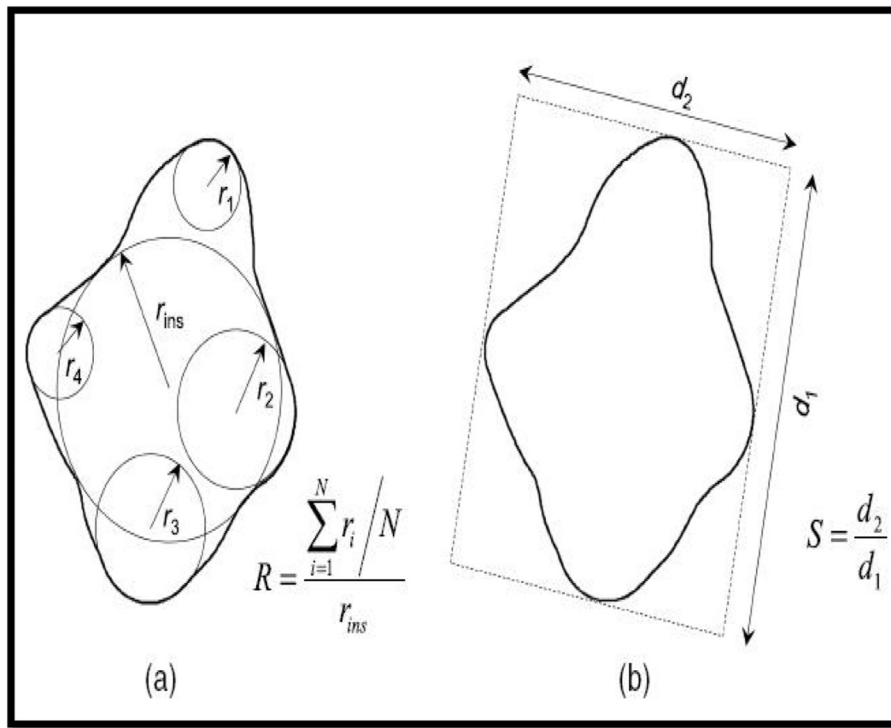


Fig. 21. Definitions (a) Roundness (b) Sphericity [117].

cross-validation. The roundness is then determined from the mean surface of the particle based on the Wadell definition [109]. They compared the results of their numerical computational geometry method with those of the manual Wadell method, the Wadell roundness [109], and sphericity, which is defined as a ratio of a diameter of an equivalent-projected-area circle to a minimum circumscribing circle diameter. Furthermore, their method is compared with the Krumbein and Sloss chart [110] shown in Fig. 20; this chart provides the Wadell roundness [109] and sphericity that is defined as a ratio of the particle width to length. Good agreement between these two methods suggests that to obtain reliable results, the images used in the image analysis should have a resolution of at least 200 pixels per circumscribing circle diameter, and the maximum departure of linear segment approximation should be <0.03% of the circumscribing circle diameter. Moreover, Hryciw, Zheng and Shetler [117] have statistically analyzed and compared their computational results of roundness and sphericity, as defined in Fig. 21,

with the visual estimation chart method [110] that was used by 38 undergraduate civil engineering students with 3D images of 20 different soil samples. However, the students, on average, underestimated the values of the roundness and sphericity. Hryciw, Zheng and Shetler [117] suggested that the main reason for the differences is that in the visual estimation, the attention of the students was drawn to the most unusual (angular and non-spherical) particles, which can lead to faulty results that do not reflect the abundance or scarcity of those particles in the image. Furthermore, Zheng and Hryciw [118] concluded that for crushed sand, the mean value of roundness is smaller than that of alluvial or glacio-fluvial sand values. Furthermore, Zheng and Hryciw [119] have recently suggested using stereophotography and image analysis to enhance the precision of the shape and size estimation by considering the three primary dimensions of soil and gravel particles. They compared their results with manual caliper and sieve measurements, as shown in Fig. 22, and excellent agreement between these two methods

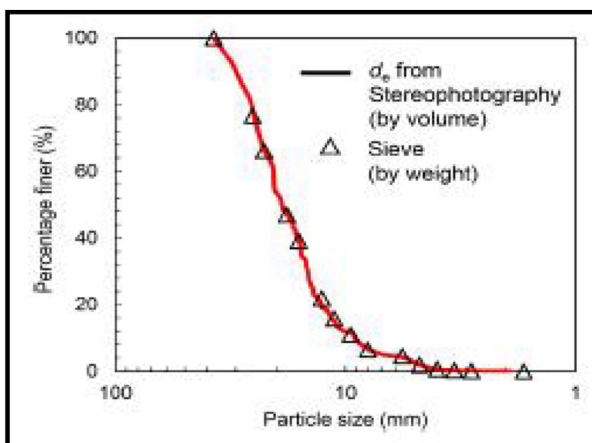


Fig. 22. Comparison between stereophotography and sieving dimensions [119].

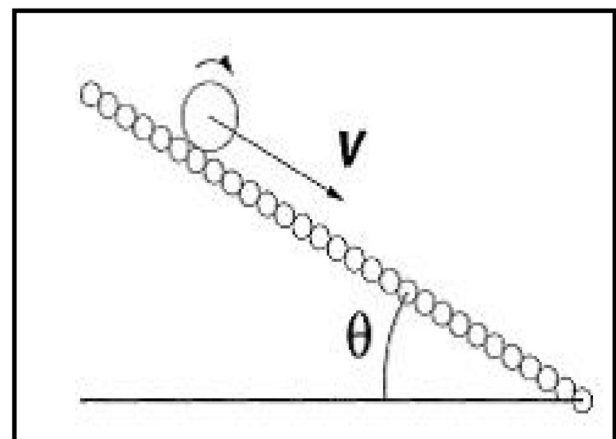
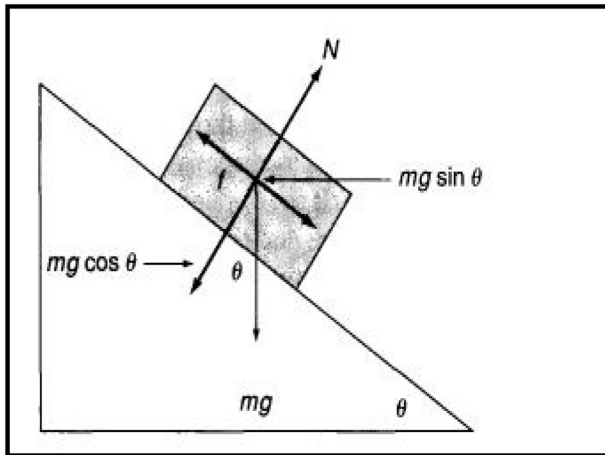


Fig. 23. Viscous friction caused by roughness to a rolling particle [127].



**Fig. 24.** Sliding of an object on an inclined plane [134].

was observed. Zheng and Hryciw [119] have also determined the 3D profile of sand and glass particles using X-ray computed tomographic imaging, as well as 2D profile imaging, concluding that even the 2D shape descriptors can be used to reasonably estimate the soil properties.

Similarly, in chemical engineering applications, the defined circularity or roundness does affect the particles flowability and granular material properties [33,120]. The aspect ratio and roundness are found to be the best shape descriptors in this field [33]. For fine powders that vary in shapes, it is suggested to obtain the probability distribution (normal distribution usually) of roundness instead of a single value [33]. Fine powders, such as Aspartame, exhibit a non-linear decrease in the static angle of repose as the roundness increases [33]. However, for powders that include irregular roundness profiles, such a conclusion might not be achieved due to the effects of cohesion and interlocking forces [33].

From the above review, it could be concluded that as the roundness increases, the angle of repose decreases [19,115], as shown in Fig. 6. The decrease in the roundness or increase in the angularity of the particles will increase the particle contact and interlocking, thereby increasing the angle of repose.

#### 4.1.2. Sphericity of particles

Like roundness, sphericity is used as a shape descriptor, as mentioned earlier. As with roundness, sphericity has various definitions and is determined using various methods [116]. A common definition

**Table 3**  
Wadell's roundness classification [111].

Description	Roundness
Very angular	<0.17
Angular	0.17–0.25
Sub-angular	0.25–0.35
Sub-rounded	0.35–0.49
Rounded	0.49–0.70
Well-rounded	>0.70

of sphericity was proposed by Wadell [109], who defined sphericity as the ratio of the diameter of an equivalent volume sphere to the diameter of the circumscribing sphere, as shown in Fig. 19. Riley and Mann [82] noticed that for glass particles, the angle of repose increased with the variation in the spherical shape; however, for extreme shape variations, like flakes, the relationship was not predictable. Barrios et al. [121] simulated the angle of repose of iron pellets in a DEM using spherical and clump shapes. The predicted angle of repose of the spherical particles was higher than the measured angle, while the predicted angle of repose of the clump particles matched closely with the experimental results. Additionally, the angles of repose were in good agreement when only the static friction coefficient of the spherical particles was reduced. Höhner, Wirtz and Scherer [122] simulated a rotating drum in a DEM to predict the dynamic angle of repose of spherical and non-spherical particles. However, they noticed that the dynamic angle of repose was greater for the non-spherical particles. The same result has been achieved in other studies [51]. Using both roundness and sphericity, Zheng and Hryciw [123] provided a clump library that contains >100,000 clumps for modelling the real shape of soil particles in DEM simulations, similar to the work conducted by Zhou, Wang and Wang [124]. Additionally, Dai et al. [125] have shown that the angle of repose decreases when the circularity and/or aspect ratio increase, and when the sphericity increases [126].

#### 4.1.3. Roughness

Both the roughness of particles and the sliding surface affect the angle of repose and friction coefficients of the particles. The roughness of a particle describes the texture relative to its radius, on a scale that is much smaller than the diameter of the particle [19]. The direct measurement of roughness is strenuous; therefore, it is usually measured relative to the length of the inter-particle contact area. For a rolling particle on a sliding surface of the same or different material, the roughness controls the viscous friction [127], as shown in Fig. 23. Senetakis, Coop and Todisco [128] measured the roughness of sand quartz minerals using white light interferometry and a Sympatec QicPic laser scanner, and the average roughness was found to be  $0.38 \pm 0.19 \mu\text{m}$ . Similar work was conducted by Yang and Baudet [129] using the power spectrum method. Miura, Maeda and Toki [39] noticed that when the roughness of the base, which the sand was piled on, increased, the angle of repose also increased; consequently, forming a heap on a frictionless base is nearly impossible. Similarly, Zaalouk and Zabady [68] proved that for different types of wheat, the angle of repose increases with the roughness of the base. Liu [7] provided similar results for sand. Additionally, Altuhafi, Coop and Georgiannou [130] noticed that the normalized elastic shear modulus increased with the surface roughness of natural sand and correlated the shape descriptors with the stiffness and critical state parameters of the soil.

#### 4.2. Particle size

As shown in Eq. (1), the angle of repose decreases when the spherical glass particle diameter increases [83]. Botz et al. [69] have shown similar results for the sand in antlions pits: the angle of repose decreased when the particle size of the sand increased. Moreover, considering the particle size distribution, as the mean particle size increases,

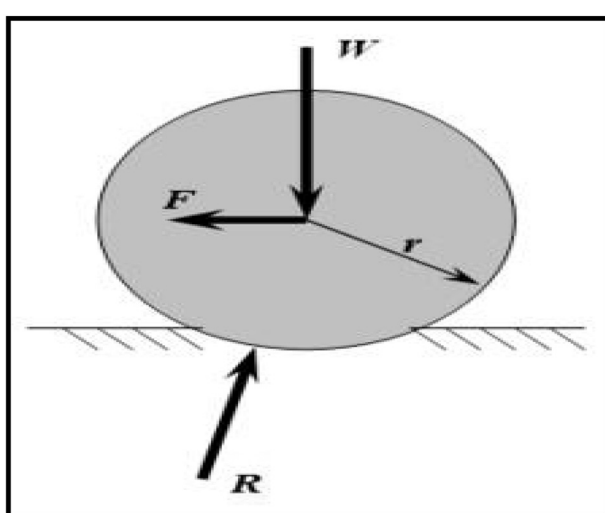


**Fig. 25.** Rolling friction of a particle (Wiki).

the angle of repose decreases [131]. Lumay et al. [132] demonstrated that when the particle sizes of rice, flours, and silicon carbide abrasives are lower than 50 µm, the cohesion between the particles tends to affect the angle of repose, i.e., as the cohesion increases, the angle of repose increases. However, for particle sizes >50 µm, the particle shape, especially the elongation, will predominate the macrobehavior of the particles. For non-uniform sediments, Yang et al. [78] noticed that when the mean sediment size increases, the angle of repose increases slightly. Moreover, it was noted that as the mean size of the material decreases, the difference between the dynamic and static angles of repose increases [133].

#### 4.3. Friction coefficients

Different types of friction coefficients influence the macro- and micro-behavior of granular materials, namely the sliding friction coefficient (both static and kinetic) and the rolling friction coefficient.

##### 4.3.1. Sliding (Coulomb) friction coefficients

The sliding friction of an object is defined as the force that resists an object as it slides or starts to slide along a surface; this force acts along the contact points between the two surfaces in an opposite direction to the possible motion [134]. This coefficient has two components (i.e., the static and kinetic coefficients). There are many other definitions, empirical laws and theories that are used to describe the sliding friction coefficients. The general form of the sliding coefficient, without rolling, plastic deformation or external loads, can be described by the inclined plane method, as shown in Fig. 24. The static friction force is proportional to the normal force, as shown in Eq. (7), and is defined as the force that is required for an object to start sliding. When the object starts moving along the sliding surface, the frictional force is called the kinetic friction force, which is also proportional to the normal force, as shown in Eq. (8). By solving the free body diagram of Fig. 24 at static conditions, the static friction coefficient can be expressed by Eq. (9). Similarly, taking into consideration the kinetic conditions and uniform acceleration equations, the kinetic friction coefficient can be expressed by Eq. (10) and is always smaller than the static friction coefficient [134].

Static friction coefficient [134]:

$$f_s \leq \mu_s \times N, \quad N = m \times g \times \cos \theta \dots \quad (7)$$

Kinetic friction coefficient [134]:

$$f_k = \mu_k \times N \dots \quad (8)$$

Solving for static friction coefficient:

$$\mu_s = \frac{\sin \theta}{\cos \theta} = \tan \theta \dots \quad (9)$$

Solving for kinetic friction coefficient:

$$\mu_k = \frac{(g \times \sin \theta) - a_x}{g \times \cos \theta}, \quad a_x = \frac{2 \times d}{\Delta t^2} \dots \quad (10)$$

where:  $f_s$  = static friction force;  $\mu_s$  = static friction coefficient;  $N$  = normal force;  $m$  = mass of the object;  $g$  = gravity acceleration;  $\theta$  = inclination angle at which the object is sliding or starts to slide;  $f_k$  = kinetic friction force;  $\mu_k$  = kinetic friction coefficient;  $a_x$  = uniform acceleration of the object;  $d$  = sliding distance of the object; and  $\Delta t^2$  = time for the object to slide along distance  $d$ .

From Eq. (9), one may conclude that the static friction coefficient is equal to the tangent of the angle of repose, but this conclusion may be true only under strict conditions and assumptions. Zhou et al. [83] reported a positive relationship between the angle of repose and the static sliding and rolling coefficients of coarse sphere glass beads, as shown in Eq. (1), and similar results were achieved by others [135,136]. Santos

et al. [137] conducted DEM simulations for a rotary drum to measure the dynamic angle of repose of rice grains and glass beads. They found that the dynamic angle of repose is affected by the sliding friction coefficient while only slightly affected by the damping or restitution coefficient. In general, the angle of repose increases with an increase in the sliding friction coefficient [54,138,139].

##### 4.3.2. Rolling friction coefficient

Rolling friction (i.e., resistance or drag) is defined as the force that resists movement of a particle rolling on a surface [140], as shown in Fig. 25. The rolling friction coefficient is much smaller than the sliding friction coefficient [140] and can be expressed in Eq. (11) as a dimensionless coefficient or in Eq. (12) as a coefficient with a dimension of length [141]. However, different models and equations are presented in the literature for specific conditions and applications [142,143]. Fukumoto, Sakaguchi and Murakami [144] conducted DEM simulations to investigate the effects of the rolling coefficient on the behavior of granular materials. The rolling friction coefficient was found to affect the rearrangement of the particles during packing, and the fabric anisotropy increased with the rolling friction coefficient. Furthermore, when the rolling friction coefficient increased, the coefficient of earth pressure (a ratio between the horizontal to vertical stresses on earth structures) at rest decreased. The rolling friction was also found to contribute to the heterogeneity in the stress distribution between particles. The authors recommended studying different particle packing methods and their effect on the rolling friction by using DEM simulations [144].

Rolling friction coefficient (dimensionless) [141]:

$$F = \mu_r \times W \dots \quad (11)$$

Rolling friction coefficient (length dimension) [141]:

$$F = \frac{b \times W}{r}, \quad \frac{b}{r} = \mu_r \dots \quad (12)$$

where:  $F$  = rolling friction force;  $\mu_r$  = rolling friction coefficient;  $W$  = normal force, as shown in Fig. 25, and  $R$  is the reaction force;  $b$  = rolling friction coefficient with a dimension of length; and  $r$  = radius of the particle or inter-particle contact length (coordination number).

Briend, Radziszewski and Pasini [54] observed that the angle of repose of soil increases when the rolling friction coefficient increases and similar results have been reported in the literature [57,83,135,136,138,145]. Markauskas and Kacianauskas [146] modeled ellipsoidal rice grains in a DEM simulation that included the rolling friction. From this work, they proved that if the rolling friction is ignored or set to zero, even with a sliding friction coefficient of 1.0, the model cannot correctly predict the angle of repose but it produces a lower angle of repose than measured. Moreover, as the rolling or sliding friction coefficients increase; the angle of repose increases, due to the associated increment of dissipation rate of kinetic energy [84].

##### 4.3.3. Angle of internal friction

Several studies have shown that the angle of internal friction is approximately equal to the angle of repose [7,39], but this conclusion is valid under very restricted conditions and assumptions, as shown earlier in Section 1.2 [21,126,147]. These restrictions are ascribed to the fact that the granular material has a uniform density and moisture content and that the particles have a uniform size [38]. Coetzee [139] conducted a large shear box test and compared the results with the angle of repose results used to calibrate a DEM simulation; however, he concluded that both the direct shear results and the angle of repose results were different. Härtl and Ooi [148] found similar results and ascribed the difference between the angle of repose and the internal friction angle to the confining effects of the rigid shear box.

#### 4.4. Coefficient of restitution (damping)

The coefficient of restitution is a measure of the energy that is transferred between the particles and the surface of impact. Numerically, an approximation of the restitution coefficient can be expressed in Eq. (13) [149]; it is simply a ratio of the rebound height of a particle to the initial height. Zhou et al. [83] reported that the angle of repose is not affected by Poisson's ratio, the elastic modulus or the restitution coefficient, and similar findings were cited elsewhere [150]. However, Santos et al. [137] reported minor effects of the restitution coefficient on the angle of repose.

Approximation of restitution coefficient [149]:

$$e = \frac{2}{v_0} \times \left( \frac{2 \times E}{m \times (1-v^2)} \right) \times \left( \frac{2 \times U_0^{\frac{5}{2}}}{15} + \frac{r_1^2 \times U_0^{\frac{3}{2}}}{3} \right)^2 \dots \quad (13)$$

where:  $e$  = restitution coefficient;  $v_0$  = impact velocity;  $E$  = elastic modulus;  $m$  = mass;  $v$  = Poisson's ratio;  $U_0$  = deformation; and  $r_1$  = permanent deformation.

#### 4.5. Number of particles

In either a physical experiment or DEM simulation, the amount of granular material or the number of particles has been found to affect the angle of repose. Miura, Maeda and Toki [39] found that the angle of repose decreases with an increase in the amount of material, and similar results have been achieved by Liu [7]. Stahl and Konietzky [151] proved, through DEM simulation, that the angle of repose decreases slightly when the amount of granular material or number of particles increased. This result was verified by physical experiments, and similar findings have also been reported by Coetze [139]. In addition, the heterogeneity and stratification of a mixture have been found, unsurprisingly, to affect the angle of repose [7,104,126]. Chik, Zamri and Vallejo [73] reported that the angle of repose for a mixture with predominantly coarse sand is greater than that for a mixture with predominantly fine sand. On a smooth base, the angle of repose is minimized for both coarse- and fine-grained sands, and the failure mode takes the form of lateral spreading.

#### 4.6. Moisture content and air flow

Zaalouk and Zabady [68] reported that the angle of repose generally increases with the moisture content of the granular material. However, in a DEM simulation, coupling with a CFD may be required to account for moisture content and fluid flow effects [152]. Derakhshani, Schott and Lodewijks [153] conducted a CFD-DEM simulation and concluded that only minor errors occur in the prediction of the angle of repose if the air flow effects are ignored during the simulation. The angle of repose is found to be increased once the water content in a material exceeded a critical value, which is ascribed to the electrostatic attraction between the water molecules and compositional minerals surfaces [154]. As part of a segregation study of wet granular material, Chou, Liao and Hsiau [155] used a rotating drum to show that the dynamic angle of repose increases with the interstitial liquid volume until a critical amount of liquid. Thereafter, the angle of repose remains constant. Additionally, similar trends have been reported between the angle of repose and liquid viscosity [156]. Later, similar results have been presented for effect of both the fluid viscosity and particle density [157], but the angle of repose decreased as the density increased. Yang et al. [78] concluded that the angle of repose in water is slightly greater than that in air.

#### 4.7. Methods of measurement

A number of comparative studies have reported a significant difference in the values of angle of repose that are obtained from different

methods or scales [53,104,158]. When using the same method, different combinations, scales, or conditions, such as the lifting speed in the hollow cylinder method or the rotating speed in the revolving drum method, will lead to different measurements of the angle of repose. For instance, when the lifting speed increases, the angle of repose decreases [7,53,159]. In the rotating drum method, when the rotating speed is increased, the angle of repose increases [160]. Grima and Wypych [161] explained that the difference in the measurements between the methods is because the relative particle velocity is different in each method. Li et al. [162] studied the effects of the container shape and lifting velocity on the angle of repose of iron ore material and found that the angle of repose decreases exponentially when the lifting velocity is increased for all the container shapes tested. They developed reliable prediction equations for estimating the angle of repose from the lifting velocity and mean particle size for each of the container shapes. Moreover, the angle of repose of the particles was found smaller in the axial center of a rotating drum than that near the walls [163].

### 5. Conclusions

This literature review highlights the importance of the angle of repose in a wide range of applications and its ability to describe and assess the macro- and micro-mechanical behavior of granular materials. The angle of repose has many definitions and methods of measurement, and each of these methods should be used to mimic the granular material behavior of a particular application. Therefore, drawing a conclusion from or conducting a comparison between different methods of measurement may be challenging because each measurement method is used to simulate a specific application.

The literature review indicates that the angle of repose has been used in different fields, such as agriculture (for the design of silos and hoppers), pharmacology (in drug production and flowability determination), geology (for the evaluation and monitoring of sand dunes and granular formations), bulk material handling, mining, civil engineering, and numerical model calibration, as well as in other applications. An important use of the angle of repose, along with the bulk density and sliding friction coefficient, is to calibrate DEM simulations, which allow the estimation and determination of the inter-particle parameters that are difficult to measure experimentally.

Several factors have been found to affect the angle of repose, such as the static sliding friction coefficient, rolling friction coefficient, coefficient of restitution, particle size and shape, amount of the material used in the measurement, and method of measurement. The reported data indicate that the angle of repose increases with the particle and impacted surface roughness, sliding and rolling friction coefficients, moisture content, deviation from roundness, and increase in the revolving drum speed. In contrast, the angle of repose decreases with the amount of material used in the measurement, the size of the particles and lifting speed of the hollow cylinder increase.

The angle of repose is not always equal to either the peak or residual internal friction angle. In direct shear tests, the factors that ensure that the angle of repose equals the residual internal friction angle are the sample preparation method and sample conditions, such as moisture content, maximum dry density, particle size, etc. Therefore, the angle of repose should be considered as an estimation of the residual internal friction angle only under certain circumstances. Although measurement of the angle of repose is fairly simple, slight differences in the sample conditions or the method of measurement will lead to erroneous results.

### 6. Recommendations for future research

Considering this literature review, the following future research is recommended:

- To determine the angle of repose, regardless of the method of measurement used, state-of-the-art methodologies (such as digital

- image analysis and processing or 3D scanning) and the “fractal dimension” [164] may be used instead of linear averaging methods, to describe the slope of the pile. The fractal dimension can then be related to the shape descriptors, material properties, and conditions of the measurements to provide a generalized fractal model that can be used to measure more precisely the angle of repose.
- The potential physico-chemical interactions, such as surface charges and force fields, among different types of materials will certainly affect the angle of repose and may be studied through molecular modelling and simulations.
  - The effects of matric suction and/or chemical potential on the angle of repose in partially saturated materials and the impact of the apparent cohesion on the formation of heaped granular materials may be studied.
  - In numerical simulations, such as DEM, a jamming model for the granular particles may be defined to study the jamming transition effect; for instance, this work can be used to numerically optimize the outlet size of silos.
  - If feasible, a correction factor or formula for the angle of repose obtained by direct or conventional methods may be developed on the basis of the outcome of new approaches to exploit the angle of repose database available in the literature (similar to the correlation developed between the angle of repose from a conical shape and the deviation in the angle of repose by Dai, Yang and Zhou [66]).
  - In engineering design processes (e.g., geotechnical design), the advantages of utilizing the angle of repose correlations over conventional laboratory and field testing can be emphasized.

## Acknowledgments

The authors gratefully acknowledge King Fahd University of Petroleum & Minerals (KFUPM), Dhahran, Saudi Arabia, for supporting this study, particularly the Department of Civil & Environmental Engineering, the Deanship of Scientific Research (Prof. Naser M. Al-Aqeeli) and Dr. Abdullah Al-Sunaidi (Chairman, Physics Department). Further, the authors appreciate the thorough and detailed comments of the anonymous specialists who reviewed this article.

## References

- [1] P. Richard, M. Nicodemi, R. Delannay, P. Ribière, D. Bideau, Slow relaxation and compaction of granular systems, *Nat. Mater.* 4 (2005) 121–128, <https://doi.org/10.1038/nmat1300>.
- [2] B. Kou, Y. Cao, J. Li, C. Xia, Z. Li, H. Dong, A. Zhang, J. Zhang, W. Kob, Y. Wang, Granular materials flow like complex fluids, *Nature* (2017) 1–13, <https://doi.org/10.1038/nature24062>.
- [3] J.F. Peters, M. Muthuswamy, J. Wibowo, A. Tordesillas, Characterization of force chains in granular material, *Phys. Rev. E* 72 (2005) 1–8, <https://doi.org/10.1103/PhysRevE.72.041307>.
- [4] D. Schulze, Measuring powder flowability: a comparison of test methods – part II, *Powder Bulk Eng.* 10 (1996) 17–28.
- [5] J. Duran, Sands, Powders, and Grains: An Introduction to the Physics of Granular Materials, Springer New York, New York, NY, 2000, <https://doi.org/10.1007/978-1-4612-0499-2>.
- [6] J.K. Mitchell, K. Soga, Fundamentals of Soil Behavior, 3rd ed. John Wiley & Sons, Inc, New Jersey, 2005, <https://doi.org/10.2136/sssaj1976.03615995004000040003x>.
- [7] Z. Liu, MS Thesis: Measuring the Angle of Repose of Granular Systems Using Hollow Cylinders, University of Pittsburgh, 2011, <http://d-scholarship.pitt.edu/6401/>.
- [8] A. Mehta, G.C. Barker, The dynamics of sand, reports, *Prog. Phys.* 57 (1994) 383–416, <https://doi.org/10.1088/0034-4885/57/4/002>.
- [9] J.K. Beddoe, Professor Dr. Henry H. Hausner, 1900–1995, Part. Part. Syst. Charact. 12 (1995), <https://doi.org/10.1002/ppsc.19950120411> (213–213).
- [10] ASTM-C1444, Standard Test Method for Measuring the Angle of Repose of Free-Flowing Mold Powders (withdrawn 2005), ASTM Int. 08.03, 2000, <https://doi.org/10.1520/C1444-00>.
- [11] J. Cain, An alternative technique for determining ANSI/CEMA standard 550 flowability ratings for granular materials, *Powder Handl. Process.* 14 (2002) 218–220, <https://www.tib.eu/en/search/id/ceaba%3ACEAB20021101527/An-alternative-technique-for-determining-ANSI-CEMA/>.
- [12] R.E. Riley, H.H. Hausner, Effect of particle size distribution on the friction in a powder mass, *Int. J. Powder Metall.* 6 (1970) 17–22, <https://www.osti.gov/scitech/biblio/4173860>.
- [13] ASTM-D6393, Standard test method for bulk solids characterization by Carr indices, J. ASTM Int. 04.09 (2014), <https://doi.org/10.1520/D6393-14>.
- [14] G.S. Riley, S. Mann, R.O. Jesse, Angle of repose of cohesive powders, *J. Powder Bulk Solids Technol.* 2 (1978) 15–18, [https://www.tib.eu/de/suchen/id/ceaba%3ACEAB1980210637/Angles-of-repose-of-cohesive-powders/?tx\\_tibsearch\\_search%5Bsearchspace%5D=tn](https://www.tib.eu/de/suchen/id/ceaba%3ACEAB1980210637/Angles-of-repose-of-cohesive-powders/?tx_tibsearch_search%5Bsearchspace%5D=tn).
- [15] K. Terzaghi, Theoretical Soil Mechanics, John Wiley & Sons, Inc., Hoboken, NJ, USA, 1943, <https://doi.org/10.1002/9780470172766>.
- [16] R.W. Day, Foundation Engineering Handbook: Design and Construction with 2009 International Building Code, 2nd ed. McGraw Hill companies, Inc., New York, 2010, <https://www.accessengineeringlibrary.com/browse/foundation-engineering-handbook-design-and-construction-with-the-2009-international-building-code-second-edition>.
- [17] J.E. Bowles, Foundation Analysis and Design, 5th ed. McGraw-Hill, Inc., Singapore, 1997, [https://doi.org/10.1016/0013-7952\(84\)90010-3](https://doi.org/10.1016/0013-7952(84)90010-3).
- [18] E.L. Nicholas, W.S. Franklin, The Elements of Physics; A College Textbook, Macmillan, Ithaca, N.Y., U.S.A., New York, 1896, <https://archive.org/details/elementsofphysic02nichuoft>.
- [19] J.C. Santamarina, G.C. Cho, Soil behaviour: the role of particle shapeSkempt. Conf., London 2004, pp. 1–14, [http://pmrl.ice.gatech.edu/tools/santamarina\\_cho\\_2004.pdf](http://pmrl.ice.gatech.edu/tools/santamarina_cho_2004.pdf).
- [20] B.M. Das, Principles of Geotechnical Engineering, 7th ed. Cengage Learning, Stanford, USA, 2010, [www.cengage.com/engineering](http://www.cengage.com/engineering).
- [21] J.R. Metcalf, Angle of repose and internal friction, *Int. J. Rock Mech. Min. Sci. Geomech. Abstr.* 3 (1966) 155–161, [https://doi.org/10.1016/0148-9062\(66\)90005-2](https://doi.org/10.1016/0148-9062(66)90005-2).
- [22] C. Lanzerstorfer, Dusts from dry off-gas cleaning: comparison of flowability determined by angle of repose and with shear cells, *Granul. Matter* 19 (2017) 58, <https://doi.org/10.1007/s10035-017-0745-2>.
- [23] C. Coulomb, Mémoires de mathématique et de physique, présentés à l'Académie royale des sciences, par divers savans & lüs dans ses assemblées, Académie R. Des. Sci. 7 (1776) 343–382, <http://www.biodiversitylibrary.org/bibliography/4360/#/summary>.
- [24] M. Rackl, F.E. Grötsch, W.A. Günther, Angle of repose revisited: when is a heap a cone?, *EPJ Web Confvol.* 140, 2017, pp. 1–4, <https://doi.org/10.1051/epjconf/201714002002>.
- [25] Z. Deng, A. Smolyanitsky, Q. Li, X.-Q. Feng, R.J. Cannara, Adhesion-dependent negative friction coefficient on chemically modified graphite at the nanoscale, *Nat. Mater.* 11 (2012) 1032–1037, <https://doi.org/10.1038/nmat3452>.
- [26] J.G. Potyondy, Skin friction between various soils and construction materials, *Géotechnique* 11 (1961) 339–353, <https://doi.org/10.1680/geot.1961.11.4.339>.
- [27] I. Noorany, Shear strength properties of some deep-sea Pelagic sediments, *Strength Test. Mar. Sediments Lab. In-Situ Meas.*, ASTM International, 100 Barr Harbor Drive, PO Box C700, West Conshohocken, PA 19428–2959 1985, pp. 1–7, <https://doi.org/10.1520/STP36338S>.
- [28] R.D. Holtz, W.D. Kovacs, An Introduction to Geotechnical Engineering, Illustrate, Prentice-Hall, Englewood Cliffs, NJ., USA, 1981, <https://trid.trb.org/view.aspx?id=214980>.
- [29] M.J. Tomlinson, R. Boorman, Foundation Design and Construction, 7th ed. Longman Group United Kingdom, 2001.
- [30] T.J. Glover, Pocket Reference, 2nd ed. Sequoia Publishing, Inc, 1997.
- [31] M. Rackl, F.E. Grötsch, M. Rusch, J. Fottner, Qualitative and quantitative assessment of 3D-scanned bulk solid heap data, *Powder Technol.* 321 (2017) 105–118, <https://doi.org/10.1016/j.powtec.2017.08.009>.
- [32] R.Y. Yang, R.P. Zou, A.B. Yu, Microdynamic analysis of particle flow in a horizontal rotating drum, *Powder Technol.* 130 (2003) 138–146, [https://doi.org/10.1016/S0032-5910\(02\)00257-7](https://doi.org/10.1016/S0032-5910(02)00257-7).
- [33] A. Bodhimage, MS Thesis: Correlation Between Physical Properties and Flowability Indicators for Fine Powders, University of Saskatchewan, 2006, <http://www.collectionscanada.gc.ca/obj/s4/f2/dsk3/SSU-07032006115722.pdf>.
- [34] J.J. Fitzpatrick, L. Aherné, Food powder handling and processing: industry problems, knowledge barriers and research opportunities, *Chem. Eng. Process. Process Intensif.* 44 (2005) 209–214, <https://doi.org/10.1016/j.cep.2004.03.014>.
- [35] H.N. Pitanga, J.-P. Gourc, O.M. Vilar, Interface shear strength of geosynthetics: evaluation and analysis of inclined plane tests, *Geotext. Geomembr.* 27 (2009) 435–446, <https://doi.org/10.1016/j.geotexmem.2009.05.003>.
- [36] L.J. Johnston, J. Goihl, G.C. Shurson, Selected additives did not improve flowability of DDGS in commercial systems, *Appl. Eng. Agric.* 25 (2009) 75–82, <https://doi.org/10.13031/2013.25422>.
- [37] G.-C. Cho, J. Dodds, J.C. Santamarina, Particle shape effects on packing density, stiffness, and strength: natural and crushed sands, *J. Geotech. Geoenviron. Eng.* 132 (2006) 591–602, [https://doi.org/10.1061/\(ASCE\)1090-0241\(2006\)132:5\(591\)](https://doi.org/10.1061/(ASCE)1090-0241(2006)132:5(591)).
- [38] E. Nelson, Measurement of the repose angle of a tablet granulation, *J. Am. Pharm. Assoc. Am. Pharm. Assoc.* 44 (1955) 435–437, <http://www.ncbi.nlm.nih.gov/pubmed/13242433>.
- [39] K. Miura, K. Maeda, S. Toki, Method of measurement for the angle of repose of sands, *Soils Found.* 37 (1997) 89–96, <http://ci.nii.ac.jp/naid/110003946069/en/>.
- [40] D.C. Shorts, K. Feitosa, Experimental measurement of the angle of repose of a pile of soft frictionless grains, *Granul. Matter* 20 (2018) 2, <https://doi.org/10.1007/s10035-017-0774-x>.
- [41] D. Geldart, E.C. Abdullah, A. Hassanpour, L.C. Nwoke, I. Wouters, Characterization of powder flowability using measurement of angle of repose, *China Particul.* 4 (2006) 104–107, [https://doi.org/10.1016/S1672-2515\(07\)60247-4](https://doi.org/10.1016/S1672-2515(07)60247-4).
- [42] O. Chukwu, F.B. Akande, Development of an apparatus for measuring angle of repose of granular materials, *Au. J. T.* 11 (2007) 62–66[https://s3.amazonaws.com/academia.edu.documents/31233818/auJournalTech\\_article10.pdf?AWSAccessKeyId=](https://s3.amazonaws.com/academia.edu.documents/31233818/auJournalTech_article10.pdf?AWSAccessKeyId=)

- AKIAIWOWYYGZ2Y53UL3A&Expires=1505508046&Signature=HRomsWPISI1PlFSIFjBXjSIPD4Q%3D&response-content-disposition=inline%3Bfilename%3DDevelopment\_of\_an\_Appara.
- [43] H. Nakashima, Y. Shioji, T. Kobayashi, S. Aoki, H. Shimizu, J. Miyasaka, K. Ohdoi, Determining the angle of repose of sand under low-gravity conditions using discrete element method, *J. Terramech.* 48 (2011) 17–26, <https://doi.org/10.1016/j.jterra.2010.09.002>.
- [44] A. Szalay, A. Kelemen, K. Pintye-Hódi, The influence of the cohesion coefficient ( $C$ ) on the flowability of different sorbitol types, *Chem. Eng. Res. Des.* 93 (2015) 349–354, <https://doi.org/10.1016/j.cherd.2014.05.008>.
- [45] R.T. Fowler, F.A. Wyatt, The effect of moisture content on the angle of repose of granular solids, *Aust. J. Chem. Eng.* (1960) 5–8.
- [46] M.G. Kleinhans, H. Markies, S.J. de Vet, A.C. in 't Veld, F.N. Postema, Static and dynamic angles of repose in loose granular materials under reduced gravity, *J. Geophys. Res.* 116 (2011), E11004, <https://doi.org/10.1029/2011JE003865>.
- [47] C.M. Dury, G.H. Ristow, J.L. Moss, M. Nakagawa, Boundary effects on the angle of repose in rotating cylinders, *Phys. Rev. E* 57 (1998) 4491–4497, <https://doi.org/10.1103/PhysRevE.57.4491>.
- [48] A. Castellanos, J.M. Valverde, A.T. Pérez, A. Ramos, P.K. Watson, Flow regimes in fine cohesive powders, *Phys. Rev. Lett.* 82 (1999) 1156–1159, <https://doi.org/10.1103/PhysRevLett.82.1156>.
- [49] X.Y. Liu, E. Specht, J. Mellmann, Experimental study of the lower and upper angles of repose of granular materials in rotating drums, *Powder Technol.* 154 (2005) 125–131, <https://doi.org/10.1016/j.powtec.2005.04.040>.
- [50] J. Mellmann, The transverse motion of solids in rotating cylinders—forms of motion and transition behavior, *Powder Technol.* 118 (2001) 251–270, [https://doi.org/10.1016/S0032-5910\(00\)00402-2](https://doi.org/10.1016/S0032-5910(00)00402-2).
- [51] H.R. Norouzi, R. Zarghami, N. Mostoufi, Insights into the granular flow in rotating drums, *Chem. Eng. Res. Des.* 102 (2015) 12–25, <https://doi.org/10.1016/j.cherd.2015.06.010>.
- [52] A.T. Salawu, M.L. Suleiman, M. Isiaka, Physical properties of *Jatropha curcas* seed, *Electron. J. Pol. Agric. Univ.* 16 (2013) 1–7, <http://www.ejpau.media.pl/volume16/issue4/art-07.html>.
- [53] E. Lajeunesse, A. Mangeney-Castelnau, J.P. Vilotte, Spreading of a granular mass on a horizontal plane, *Phys. Fluids* 16 (2004) 2371, <https://doi.org/10.1063/1.1736611>.
- [54] R. Briand, P. Radziszewski, D. Pasini, Virtual soil calibration for wheel-soil interaction simulations using the discrete-element method, *Can. Aeronaut. Sp. J.* 57 (2011) 59–64, <https://doi.org/10.5589/q11-009>.
- [55] H.T. Chou, C.F. Lee, Y.C. Chung, S.S. Hsiao, Discrete element modelling and experimental validation for the falling process of dry granular steps, *Powder Technol.* 231 (2012) 122–134, <https://doi.org/10.1016/j.powtec.2012.08.001>.
- [56] C.M. Wensrich, A. Katterfeld, Rolling friction as a technique for modelling particle shape in DEM, *Powder Technol.* 217 (2012) 409–417, <https://doi.org/10.1016/j.powtec.2011.10.057>.
- [57] S.M. Derakhshani, D.L. Schott, G. Lodewijks, Micro-macro properties of quartz sand: experimental investigation and DEM simulation, *Powder Technol.* 269 (2015) 127–138, <https://doi.org/10.1016/j.powtec.2014.08.072>.
- [58] H.M. Al-Hashemi, A.A.H. Balkhary, Correlation between California bearing ratio (CBR) and angle of repose of granular soil, *Electron. J. Geotech. Eng.* 21 (2016) 5655–5660, <http://www.ejege.com/2016/Ppr2016.0530ma.pdf>.
- [59] G. Biroli, Jamming: a new kind of phase transition? *Nat. Phys.* 3 (2007) 222–223, <https://doi.org/10.1038/nphys580>.
- [60] A. Janda, I. Zuriguel, A. Garcimartín, L.A. Pugnaloni, D. Maza, Jamming and critical outlet size in the discharge of a two-dimensional silo, *Europhys. Lett.* 84 (2008) 1–6, <https://doi.org/10.1209/0295-5075/84/44002>.
- [61] I. Zuriguel, A. Garcimartín, D. Maza, L.A. Pugnaloni, J.M. Pastor, Jamming during the discharge of granular matter from a silo, *Phys. Rev. E* 71 (2005) 1–9, <https://doi.org/10.1103/PhysRevE.71.051303>.
- [62] J. Frączek, A. Złobiecki, J. Zemanek, Assessment of angle of repose of granular plant material using computer image analysis, *J. Food Eng.* 83 (2007) 17–22, <https://doi.org/10.1016/j.jfoodeng.2006.11.028>.
- [63] M. Rackl, K.J. Hanley, A methodical calibration procedure for discrete element models, *Powder Technol.* 307 (2017) 73–83, <https://doi.org/10.1016/j.powtec.2016.11.048>.
- [64] European Federation of Materials Handling, FEM 2.582: General Properties of Bulk Materials and Their Symbolization (1991–11), 1991.
- [65] M.Y. Matsuo, D. Nishiura, H. Sakaguchi, Geometric effect of angle of repose revisited, *Granul. Matter* 16 (2014) 441–447, <https://doi.org/10.1007/s10035-014-0489-1>.
- [66] B.-B. Dai, J. Yang, C.-Y. Zhou, Micromechanical origin of angle of repose in granular materials, *Granul. Matter* 19 (2017), 24. <https://doi.org/10.1007/s10035-017-0709-6>.
- [67] A. Wójcik, P. Klapa, B. Mitka, J. Śladek, The use of the photogrammetric method for measurement of the repose angle of granular materials, *Measurement* 115 (2018) 19–26, <https://doi.org/10.1016/j.measurement.2017.10.005>.
- [68] A.K. Zaalouk, F.I. Zabady, Effect of moisture content on angle of repose and friction coefficient of wheat grain, *Misr. J. Agric. Eng.* 26 (2009) 418–427, <http://www.mjae.eg.net/pdf/2009/jan/22.pdf>.
- [69] J.T. Botz, C. Loudon, J.B. Barger, J.S. Olafsen, D.W. Steeples, Effects of slope and particle size on ant locomotion: implications for choice of substrate by ants, *J. Kansas Entomol. Soc.* 76 (2003) 426–435, <http://www.jstor.org/stable/25086130>.
- [70] P. Evesque, J. Rajchenbach, Instability in a sand heap, *Phys. Rev. Lett.* 62 (1989) 44–46, <https://doi.org/10.1103/PhysRevLett.62.44>.
- [71] J. Lee, H.J. Herrmann, Angle of repose and angle of marginal stability: molecular dynamics of granular particles, *J. Phys. A Math. Gen.* 26 (1993) 373–383, <https://doi.org/10.1088/0305-4470/26/2/021>.
- [72] K.A. Holsapple, Modeling granular material flows: the angle of repose, fluidization and the cliff collapse problem, *Planet. Space Sci.* 82–83 (2013) 11–26, <https://doi.org/10.1016/j.pss.2013.03.001>.
- [73] Z. Chik, L.E. Vallejo, Characterization of the angle of repose of binary granular materials, *Can. Geotech. J.* 42 (2005) 683–692, <https://doi.org/10.1139/t04-118>.
- [74] M. Ghazavi, M. Hosseini, M. Mollanouri, A comparison between angle of repose and friction angle of sand, *12th Int. Conf. Int. Assoc. Comput. Methods Adv. Geomech.*, Goa, India 2008, pp. 1272–1275, <https://pdfs.semanticscholar.org/e444/d9ce898fb10bea5ee852c982c1bf6d285e2f.pdf>.
- [75] Z. Yizheng, X. Baoling, Under water angle of rest for non-cohesive sediment, *Int. J. Hydrogen Energy* 14 (1996) 56–59.
- [76] S. Yuliang, L. Jing, Z. Yizheng, H. Changwei, Y. Jinyan, Calculation of angle of repose and dry density of sediment, *Eng. J. Wuhan Univ.* 40 (2007) 14–17.
- [77] L. Yang, B. Shi, Y. Guo, Study on dynamic angle of repose for submarine pipeline with spoiler on sandy seabed, *J. Pet. Explor. Prod. Technol.* 2 (2012) 229–236, <https://doi.org/10.1007/s13202-012-0037-7>.
- [78] F. Yang, X. Liu, K. Yang, S. Cao, Study on the angle of repose of nonuniform sediment, *J. Hydron. Ser. B* 21 (2009) 685–691, [https://doi.org/10.1016/S1001-6058\(08\)60200-0](https://doi.org/10.1016/S1001-6058(08)60200-0).
- [79] E. Kvoll, J.G. Venditti, R.W. Bradley, C. Winter, Observations of coherent flow structures over sub-aqueous high- and low-angle dunes, *J. Geophys. Res. Earth Surf.* (2017) 1–56, <https://doi.org/10.1002/2017JF004356>.
- [80] V. Meyer, A. Pisch, K. Penttilä, P. Koukkari, Computation of steady state thermochemistry in rotary kilns: application to the cement clinker manufacturing process, *Chem. Eng. Res. Des.* 115 (2016) 335–347, <https://doi.org/10.1016/j.cherd.2016.08.007>.
- [81] C.-C. Liao, A study of the effect of liquid viscosity on density-driven wet granular segregation in a rotating drum, *Powder Technol.* 325 (2018) 632–638, <https://doi.org/10.1016/j.powtec.2017.11.004>.
- [82] G.S. Riley, G.R. Mann, Effects of particle shape on angles of repose and bulk densities of a granular solid, *Mater. Res. Bull.* 7 (1972) 163–169, [https://doi.org/10.1016/0025-5408\(72\)90273-5](https://doi.org/10.1016/0025-5408(72)90273-5).
- [83] Y.C. Zhou, B.H. Xu, A.B. Yu, P. Zulli, An experimental and numerical study of the angle of repose of coarse spheres, *Powder Technol.* 125 (2002) 45–54, [https://doi.org/10.1016/S0032-5910\(01\)00520-4](https://doi.org/10.1016/S0032-5910(01)00520-4).
- [84] C. Li, T. Honeyands, D. O'Dea, R. Moreno-Atanasio, The angle of repose and size segregation of iron ore granules: DEM analysis and experimental investigation, *Powder Technol.* 320 (2017) 257–272, <https://doi.org/10.1016/j.powtec.2017.07.045>.
- [85] K. Pye, H. Tsoar, Aeolian Sand and Sand Dunes, Springer, Berlin, Heidelberg, 2009, <https://doi.org/10.1007/978-3-540-85910-9>.
- [86] J.P. Bardet, M. Kapuskar, The liquefaction sand boils in the San Francisco Marina district during the 1989 Loma Prieta earthquake, *Second Int. Conf. Recent Adv. Geotech. Earthq. Eng. Soil Dyn.* University of Missouri–Rolla, St. Louis, Missouri 1991, pp. 1687–1691, <http://scholarsmine.mst.edu/irageesd/2icragesd/session13/19>.
- [87] G. Toschkoff, S. Just, A. Funke, D. Djuric, K. Knop, P. Kleinebudde, G. Scharrer, J.G. Khinast, Spray models for discrete element simulations of particle coating processes, *Chem. Eng. Sci.* 101 (2013) 603–614, <https://doi.org/10.1016/j.ces.2013.06.051>.
- [88] M. Adedokun, B. Onah, A. Attama, Physico-mechanical and release properties of sustained release artesunate tablets in hydroxypropyl methylcellulose matrix, *Int. J. Appl. Pharm.* 10 (2018) 103–108, <https://doi.org/10.22159/ijap.2018v10i1.22918>.
- [89] D. Train, Some aspects of the property of angle of repose of powders, *J. Pharm. Pharmacol.* 10 (1958) 127T–135T, <https://doi.org/10.1111/j.2042-7158.1958.tb10391.x>.
- [90] C. Atwood-Stone, A.S. McEwen, Measuring dynamic angle of repose in low gravity environments using martian sand dunes, *44th Lunar Planet. Sci. Conf.*, LPI Contribution, Woodlands, Texas 2013, pp. 1719–1727, <http://adsabs.harvard.edu/abs/2013LPI...44.1727A>.
- [91] G.R. Hancock, D. Crawter, S.G. Fityus, J. Chandler, T. Wells, The measurement and modelling of rill erosion at angle of repose slopes in mine spoil, *Earth Surf. Process. Landf.* 33 (2008) 1006–1020, <https://doi.org/10.1002/esp.1585>.
- [92] C.J. Coetzee, Review: calibration of the discrete element method, *Powder Technol.* 310 (2017) 104–142, <https://doi.org/10.1016/j.powtec.2017.01.015>.
- [93] A. Grima, D. Hastie, D. Curry, P. Wypych, R. LaRoche, The beginning of a new era in design: calibrated discrete element modelling, *Aust. Bulk Handl. Rev.* (2011) 14–21, [https://www.edemsimulation.com/content/uploads/2012/01/BMEA\\_ABHR\\_SeptOct\\_14-21.pdf](https://www.edemsimulation.com/content/uploads/2012/01/BMEA_ABHR_SeptOct_14-21.pdf).
- [94] S. Wangchai, D.B. Hastie, P.W. Wypych, The simulation of particle flow mechanisms in dustiness testers, *11th Int. Conf. Bulk Mater. Storage, Handl. Transp.* University of Newcastle, Australia 2013, pp. 1–10, <http://ro.uow.edu.au/eispapers/1936>.
- [95] E.G. Nezami, Y.M.A. Hashash, D. Zhao, J. Ghaboussi, Simulation of front end loader bucket-soil interaction using discrete element method, *Int. J. Numer. Anal. Methods Geomech.* 31 (2007) 1147–1162, <https://doi.org/10.1002/nag.594>.
- [96] S.C. Thakur, H. Ahmadian, J. Sun, J.Y. Ooi, An experimental and numerical study of packing, compression, and caking behaviour of detergent powders, *Particuology* 12 (2014) 2–12, <https://doi.org/10.1016/j.partic.2013.06.009>.
- [97] A. Weuster, S. Strege, L. Brendel, H. Zetzener, D.E. Wolf, A. Kwade, Shear flow of cohesive powders with contact crystallization: experiment, model and calibration, *Granul. Matter* 17 (2015) 271–286, <https://doi.org/10.1007/s10035-015-0555-3>.
- [98] M. Khanal, M. Elmouttie, D. Adhikary, Effects of particle shapes to achieve angle of repose and force displacement behaviour on granular assembly, *Adv. Powder Technol.* 28 (2017) 1972–1976, <https://doi.org/10.1016/j.apt.2017.04.016>.

- [99] Z. Syed, M. Tekeste, D. White, A coupled sliding and rolling friction model for DEM calibration, *J. Terramech.* 72 (2017) 9–20, <https://doi.org/10.1016/j.jterra.2017.03.003>.
- [100] L. Wang, R. Li, B. Wu, Z. Wu, Z. Ding, Determination of the coefficient of rolling friction of an irregularly shaped maize particle group using physical experiment and simulations, *Particuology* (2017) 1–11, <https://doi.org/10.1016/j.partic.2017.06.003>.
- [101] H. Wei, L. Zan, Y. Li, Z. Wang, H. Saxén, Y. Yu, Numerical and experimental studies of corn particle properties on the forming of pile, *Powder Technol.* 321 (2017) 533–543, <https://doi.org/10.1016/j.powtec.2017.08.051>.
- [102] R. Cabisco, J.H. Finke, A. Kwade, Calibration and interpretation of DEM parameters for simulations of cylindrical tablets with multi-sphere approach, *Powder Technol.* 327 (2018) 232–245, <https://doi.org/10.1016/j.powtec.2017.12.041>.
- [103] Z. Chen, J. Yu, D. Xue, Y. Wang, Q. Zhang, L. Ren, An approach to and validation of maize seed-assembly modelling based on the discrete element method, *Powder Technol.* (2018) 1–48, <https://doi.org/10.1016/j.powtec.2017.12.007>.
- [104] L. Brezzi, S. Cola, F. Gabrieli, G. Gidoni, Spreading of kaolin and sand mixtures on a horizontal plane: physical experiments and SPH numerical modelling, *Procedia Eng.* 175 (2017) 197–203, <https://doi.org/10.1016/j.proeng.2017.01.008>.
- [105] G. Lu, J.R. Third, C.R. Müller, Discrete element models for non-spherical particle systems: from theoretical developments to applications, *Chem. Eng. Sci.* 127 (2015) 425–465, <https://doi.org/10.1016/j.ces.2014.11.050>.
- [106] J. Zheng, R.D. Hryciw, Roundness and sphericity of soil particles in assemblies by computational geometry, *J. Comput. Civ. Eng.* 30 (2016), [https://doi.org/10.1061/\(ASCE\)CP.1943-5487.0000528](https://doi.org/10.1061/(ASCE)CP.1943-5487.0000528).
- [107] K. Kumar, K. Soga, J.-Y. Delenne, F. Radjai, Modelling transient dynamics of granular slopes: MPM and DEM, *Procedia Eng.* 175 (2017) 94–101, <https://doi.org/10.1016/j.proeng.2017.01.032>.
- [108] U. Ulusoy, M. Yekeler, C. Hıçyılmaz, Determination of the shape, morphological and wettability properties of quartz and their correlations, *Miner. Eng.* 16 (2003) 951–964, <https://doi.org/10.1016/j.mineng.2003.07.002>.
- [109] H. Wadell, Volume, shape, and roundness of rock particles, *J. Geol.* 40 (1932) 443–451, <https://doi.org/10.1086/623964>.
- [110] W.C. Krumbein, LL. Sloss, in: W.H. Freeman (Ed.), *Stratigraphy and Sedimentation*, 2nd ed., 1963 [http://journals.lww.com/soilsci/citation/1951/05000/stratigraphy\\_and\\_sedimentation.19.aspx](http://journals.lww.com/soilsci/citation/1951/05000/stratigraphy_and_sedimentation.19.aspx) (San Francisco).
- [111] M.C. Powers, A new roundness scale for sedimentary particles, *SEPM J. Sediment. Res.* 23 (1953) 117–119, <https://doi.org/10.1306/D4269567-2B26-11D7-8648000102C1865D>.
- [112] Z. Li, J. Yang, X. Xu, X. Xu, W. Yu, X. Yue, C. Sun, Particle shape characterization of fluidized catalytic cracking catalyst powders using the mean value and distribution of shape factors, *Adv. Powder Technol.* 13 (2002) 249–263, <https://doi.org/10.1163/15685520232025435>.
- [113] T. Youd, Factors controlling maximum and minimum densities of sandsEval. Relat. Density Its Role Geotech. Proj. Involv. Cohesionless Soils, ASTM International, 100 Barr Harbor Drive, PO Box C700, West Conshohocken, PA 19428-2959 1973, pp. 98–112, <https://doi.org/10.1520/STP37866S>.
- [114] ASTM-D2487, Standard practice for classification of soils for engineering purposes (unified soil classification system), *J. ASTM Int.* 04.08 (2011) 1–12, <https://doi.org/10.1520/D2487-11>.
- [115] A. Cheshomi, A. Fakher, C.J.F.P. Jones, A correlation between friction angle and particle shape metrics in Quaternary coarse alluvia, *Q. J. Eng. Geol. Hydrogeol.* 42 (2009) 145–155, <https://doi.org/10.1144/1470-9236/07-052>.
- [116] J. Zheng, R.D. Hryciw, Traditional soil particle sphericity, roundness and surface roughness by computational geometry, *Géotechnique* 65 (2015) 494–506, <https://doi.org/10.1680/geot.14.P.192>.
- [117] R.D. Hryciw, J. Zheng, K. Shetler, Particle roundness and sphericity from images of assemblies by chart estimates and computer methods, *J. Geotech. Geoenviron. Eng.* 142 (2016), 4016038, [https://doi.org/10.1061/\(ASCE\)GT.1943-5606.0001485](https://doi.org/10.1061/(ASCE)GT.1943-5606.0001485).
- [118] J. Zheng, R.D. Hryciw, A corner preserving algorithm for realistic DEM soil particle generation, *Granul. Matter* 18 (2016), 84. <https://doi.org/10.1007/s10035-016-0679-0>.
- [119] J. Zheng, R.D. Hryciw, Soil particle size and shape distributions by stereophotography and image analysis, *Geotech. Test. J.* 40 (2017), 20160165. <https://doi.org/10.1520/GTJ20160165>.
- [120] N. Gui, X. Yang, J. Tu, S. Jiang, Effect of roundness on the discharge flow of granular particles, *Powder Technol.* 314 (2017) 140–147, <https://doi.org/10.1016/j.powtec.2016.09.056>.
- [121] G.K.P. Barrios, R.M. de Carvalho, A. Kwade, L.M. Tavares, Contact parameter estimation for DEM simulation of iron ore pellet handling, *Powder Technol.* 248 (2013) 84–93, <https://doi.org/10.1016/j.powtec.2013.01.063>.
- [122] D. Höhner, S. Wirtz, V. Scherer, A study on the influence of particle shape and shape approximation on particle mechanics in a rotating drum using the discrete element method, *Powder Technol.* 253 (2014) 256–265, <https://doi.org/10.1016/j.powtec.2013.11.023>.
- [123] J. Zheng, R.D. Hryciw, An image based clump library for DEM simulations, *Granul. Matter* 19 (2017), 26. <https://doi.org/10.1007/s10035-017-0713-x>.
- [124] B. Zhou, J. Wang, H. Wang, Three-dimensional sphericity, roundness and fractal dimension of sand particles, *Géotechnique* (2017) 1–13, <https://doi.org/10.1680/geot.16.P.207>.
- [125] B.-B. Dai, J. Yang, C.-Y. Zhou, W. Zhang, Effect of particle shape on the formation of sandpile, *Proc. 7th Int. Conf. Discret. Elem. Methods* 2017, pp. 767–776, <https://doi.org/10.1007/978-981-10-1926-5-79>.
- [126] H.G. Matuttis, S. Lüding, H.J. Herrmann, Discrete element simulations of dense packings and heaps made of spherical and non-spherical particles, *Powder Technol.* 109 (2000) 278–292, [https://doi.org/10.1016/S0032-5910\(99\)00243-0](https://doi.org/10.1016/S0032-5910(99)00243-0).
- [127] D.E. Wolf, Friction in granular media, *Phys. Dry Granul. Media*, Springer Netherlands, Dordrecht 1998, pp. 441–464, [https://doi.org/10.1007/978-94-017-2653-5\\_32](https://doi.org/10.1007/978-94-017-2653-5_32).
- [128] K. Senetakis, M.R. Coop, M.C. Todisco, The inter-particle coefficient of friction at the contacts of Leighton Buzzard sand quartz minerals, *Soils Found.* 53 (2013) 746–755, <https://doi.org/10.1016/j.sandf.2013.08.012>.
- [129] H. Yang, B.A. Baudet, Characterisation of the roughness of sand particles, *Procedia Eng.* 158 (2016) 98–103, <https://doi.org/10.1016/j.proeng.2016.08.412>.
- [130] F.N. Altuhafi, M.R. Coop, V.N. Georgiannou, Effect of particle shape on the mechanical behavior of natural sands, *J. Geotech. Geoenviron. Eng.* 142 (2016), 4016071, [https://doi.org/10.1061/\(ASCE\)GT.1943-5606.0001569](https://doi.org/10.1061/(ASCE)GT.1943-5606.0001569).
- [131] H. Lu, X. Guo, Y. Liu, X. Gong, Effect of particle size on flow mode and flow characteristics of pulverized coal, *Kona Powder Part. J.* 32 (2015) 143–153, <https://doi.org/10.14356/kona.2015002>.
- [132] G. Lumay, F. Boschin, K. Traina, S. Bontempi, J.-C. Remy, R. Cloots, N. Vandewalle, Measuring the flowing properties of powders and grains, *Powder Technol.* 224 (2012) 19–27, <https://doi.org/10.1016/j.powtec.2012.02.015>.
- [133] L.C. dos Santos, R. Condotta, M. do C. Ferreira, Flow properties of coarse and fine sugar powders, *J. Food Process Eng.* (2017), e12648. <https://doi.org/10.1111/jfpe.12648>.
- [134] D. Loyd, *Physics laboratory manual*, 4th ed. Cengage Learning, Boston, MA, USA, 2014, [https://books.google.com.sa/books?id=en&lr=&id=pZUWAAAQBAJ&oi=fnd&pg=PR3&dq=physics+Laboratory+Manual&ots=4zNlIxNT&sig=JB2E70Q9UW0d7s023hw01b5cy8&redir\\_esc=y#v=onepage&q=physicsLaboratory Manual&f=false](https://books.google.com.sa/books?id=en&lr=&id=pZUWAAAQBAJ&oi=fnd&pg=PR3&dq=physics+Laboratory+Manual&ots=4zNlIxNT&sig=JB2E70Q9UW0d7s023hw01b5cy8&redir_esc=y#v=onepage&q=physicsLaboratory Manual&f=false).
- [135] S. Just, G. Toschkoff, A. Funke, D. Djuric, G. Scharrer, J. Khinast, K. Knop, P. Kleinebudde, Experimental analysis of tablet properties for discrete element modeling of an active coating process, *AAPS PharmSciTech* 14 (2013) 402–411, <https://doi.org/10.1208/s12249-013-9925-5>.
- [136] M. Combarros, H.J. Feise, H. Zetzemer, A. Kwade, Segregation of particulate solids: experiments and DEM simulations, *Particuology* 12 (2014) 25–32, <https://doi.org/10.1016/j.partic.2013.04.005>.
- [137] D.A. Santos, M.A.S. Barrozo, C.R. Duarte, F. Weigler, J. Mellmann, Investigation of particle dynamics in a rotary drum by means of experiments and numerical simulations using DEM, *Adv. Powder Technol.* 27 (2016) 692–703, <https://doi.org/10.1016/j.ap.2016.02.027>.
- [138] H. Chen, Y.L. Liu, X.Q. Zhao, Y.G. Xiao, Y. Liu, Numerical investigation on angle of repose and force network from granular pile in variable gravitational environments, *Powder Technol.* 283 (2015) 607–617, <https://doi.org/10.1016/j.powtec.2015.05.017>.
- [139] C.J. Coetze, Calibration of the discrete element method and the effect of particle shape, *Powder Technol.* 297 (2016) 50–70, <https://doi.org/10.1016/j.powtec.2016.04.003>.
- [140] W.G. Peck, *Elements of Mechanics: For the Use of Colleges, Academies, and High Schools*, 1st ed. A. S. Barnes & Burr, New York, 1859, [https://books.google.com.sa/books?id=orMEAAAAYA&oe=UTF-8&redir\\_esc=y](https://books.google.com.sa/books?id=orMEAAAAYA&oe=UTF-8&redir_esc=y).
- [141] R.C. Hibbeler, *Engineering Mechanics - Statics and Dynamics*, 11th ed. Prentice Hall, 2007.
- [142] X. Tan, A. Modafe, R. Ghodssi, Measurement and modeling of dynamic rolling friction in linear microball bearings, *J. Dyn. Syst. Meas. Control.* 128 (2006) 891–898, <https://doi.org/10.1115/1.2362786>.
- [143] L. Vozdecký, J. Bartoš, J. Musilová, Rolling friction—models and experiment. An undergraduate student project, *Eur. J. Phys.* 35 (2014) 1–16, <https://doi.org/10.1088/0143-0807/35/5/05004>.
- [144] Y. Fukumoto, H. Sakaguchi, A. Murakami, The role of rolling friction in granular packing, *Granul. Matter* 15 (2013) 175–182, <https://doi.org/10.1007/s10035-013-0398-8>.
- [145] R.N. Cunha, K.G. Santos, R.N. Lima, C.R. Duarte, M.A.S. Barrozo, Repose angle of monoparticles and binary mixture: an experimental and simulation study, *Powder Technol.* 303 (2016) 203–211, <https://doi.org/10.1016/j.powtec.2016.09.023>.
- [146] D. Markauskas, R. Kačianauskas, Investigation of Rice grain flow by multi-sphere particle model with rolling resistance, *Granul. Matter* 13 (2011) 143–148, <https://doi.org/10.1007/s10035-010-0196-5>.
- [147] K. Terzaghi, R.B. Peck, *Soil mechanics in engineering practice*, SpringerReference, Springer-Verlag, Berlin/Heidelberg 1948, p. 566, [https://doi.org/10.1007/SpringerReference\\_4898](https://doi.org/10.1007/SpringerReference_4898).
- [148] J. Härtl, J.Y. Ooi, Experiments and simulations of direct shear tests: porosity, contact friction and bulk friction, *Granul. Matter* 10 (2008) 263–271, <https://doi.org/10.1007/s10035-008-0085-3>.
- [149] J.D. Armstrong, N. Collings, P.J. Shayler, Trajectory of particles rebounding off plane targets, *AIAA J.* 22 (1984) 214–218, <https://doi.org/10.2514/3.48439>.
- [150] Z. Yan, S.K. Wilkinson, E.H. Stitt, M. Marigo, Discrete element modelling (DEM) input parameters: understanding their impact on model predictions using statistical analysis, *Comput. Mech.* 2 (2015) 283–299, <https://doi.org/10.1007/s40571-015-0056-5>.
- [151] M. Stahl, H. Konietzky, Discrete element simulation of ballast and gravel under special consideration of grain-shape, grain-size and relative density, *Granul. Matter* 13 (2011) 417–428, <https://doi.org/10.1007/s10035-010-0239-y>.
- [152] M. Pezo, L. Pezo, A. Jovanović, B. Lončar, R. Čolović, DEM/CFD approach for modeling granular flow in the revolving static mixer, *Chem. Eng. Res. Des.* 109 (2016) 317–326, <https://doi.org/10.1016/j.cherd.2016.02.003>.
- [153] S.M. Derakhshan, D.L. Schott, G. Lodewijks, Calibrating the microscopic properties of quartz sand with coupled CFD-DEM framework, *Eng. Comput.* 33 (2016) 1141–1160, <https://doi.org/10.1007/EC-04-2015-0105>.
- [154] Y. Jin, H. Lu, X. Guo, X. Gong, Effect of water addition on flow properties of lignite particles, *Chem. Eng. Res. Des.* (2017), <https://doi.org/10.1016/j.cherd.2017.11.012>.

- [155] S.H. Chou, C.C. Liao, S.S. Hsiau, An experimental study on the effect of liquid content and viscosity on particle segregation in a rotating drum, *Powder Technol.* 201 (2010) 266–272, <https://doi.org/10.1016/j.powtec.2010.04.009>.
- [156] S.H. Chou, C.C. Liao, S.S. Hsiau, The effect of interstitial fluid viscosity on particle segregation in a slurry rotating drum, *Phys. Fluids* 23 (2011) 1–10, <https://doi.org/10.1063/1.3623275>.
- [157] H.T. Chou, S.H. Chou, S.S. Hsiau, The effects of particle density and interstitial fluid viscosity on the dynamic properties of granular slurries in a rotating drum, *Powder Technol.* 252 (2014) 42–50, <https://doi.org/10.1016/j.powtec.2013.10.034>.
- [158] P.C. Rousé, Comparison of methods for the measurement of the angle of repose of granular materials, *Geotech. Test. J.* 37 (2014), 20120144. <https://doi.org/10.1520/GTJ20120144>.
- [159] T. Roessler, A. Katterfeld, Scalability of angle of repose tests for the calibration of DEM parameters. ICBMH2016 Conf., the. Barton, ACT: Engineers, Australia 2016, pp. 201–211, <http://search.informit.com.au/documentSummary;dn=292983284289534;res=IELENG>.
- [160] P. Frankowski, M. Morgeneyer, Calibration and validation of DEM rolling and sliding friction coefficients in angle of repose and shear measurementsAIP Conf. Proc. 7th Int. Conf. Micromechanics Granul. Media, Sydney, Australia 2013, pp. 851–854, <https://doi.org/10.1063/1.4812065>.
- [161] A.P. Grima, P.W. Wypych, Discrete element simulations of granular pile formation, *Eng. Comput.* 28 (2011) 314–339, <https://doi.org/10.1108/02644401111118169>.
- [162] T. Li, Y. Peng, Z. Zhu, Z. Yu, Z. Yin, Effect of the lifting velocity and container shape on angle of repose of iron ore particles, *Adv. Mater. Sci. Eng.* 2017 (2017) 1–11, <https://doi.org/10.1155/2017/3405432>.
- [163] S. Yang, Y. Sun, L. Zhang, J.W. Chew, Segregation dynamics of a binary-size mixture in a three-dimensional rotating drum, *Chem. Eng. Sci.* 172 (2017) 652–666, <https://doi.org/10.1016/j.ces.2017.07.019>.
- [164] B. Mandelbrot, How long is the coast of Britain? Statistical self-similarity and fractional dimension, *Science* 156 (1967) 636–638, <https://doi.org/10.1126/science.156.3775.636>.



**Hamzah M. Beakawi Al-Hashemi** is a Civil (Geotechnical) Engineer. In 2012, he gained his B.Sc. degree from the University of Khartoum in Sudan. Hamzah has worked for three (3) years on Saudi ARAMCO CSD Geotechnical projects as a Geotechnical reporting and design Engineer. Currently, he is a postgraduate researcher at the Civil and Environmental Engineering Department, King Fahd University of Petroleum and Minerals (KFUPM), Dhahran, Saudi Arabia. His postgraduate studies are mainly focusing on unsaturated soil mechanics, granular material behaviour, slope stability, foundation design, DEM and FEM, and molecular/Nano simulation in Geotechnical and Geoenvironmental applications.



**Omar S. Baghabra Al-Amoudi** is currently the Dean of Educational Services and a Professor in the Department of Civil & Environmental Engineering at King Fahd University of Petroleum and Minerals (KFUPM), Saudi Arabia. Prof. Al-Amoudi obtained his BSc., MSc. and Ph.D. degrees (All with the first honour) from KFUPM in 1982, 1985 and 1992, respectively. He was one of the founding members of the American Concrete Institute-Saudi Arabia Chapter (ACI-SAC). Prof. Al-Amoudi has authored >180 papers in reputed journals and conferences. He won three regional awards and one international (CANMET-ACI) award. He has been the Editor-in-Chief of the Arabic Journal of Building Technology.